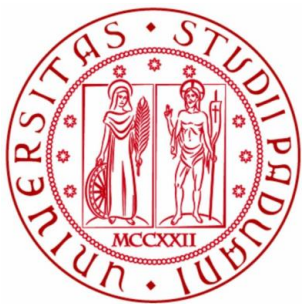




EUV polarimetry in laboratory: thin film characterization and EUV phase retarder reflector development

Paola Zuppella





Palazzo Bo



Anatomical theatre



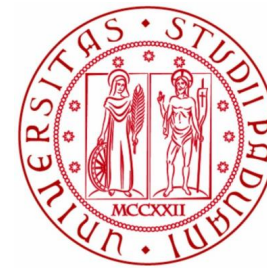
St Anthony Cathedral



<https://www.dei.unipd.it>

<http://www.pd.ifn.cnr.it>

University of Padova
Department of Information Engineering



National Research Council (Italy)
Institute of Photonics and Nanotechnologies
Padova

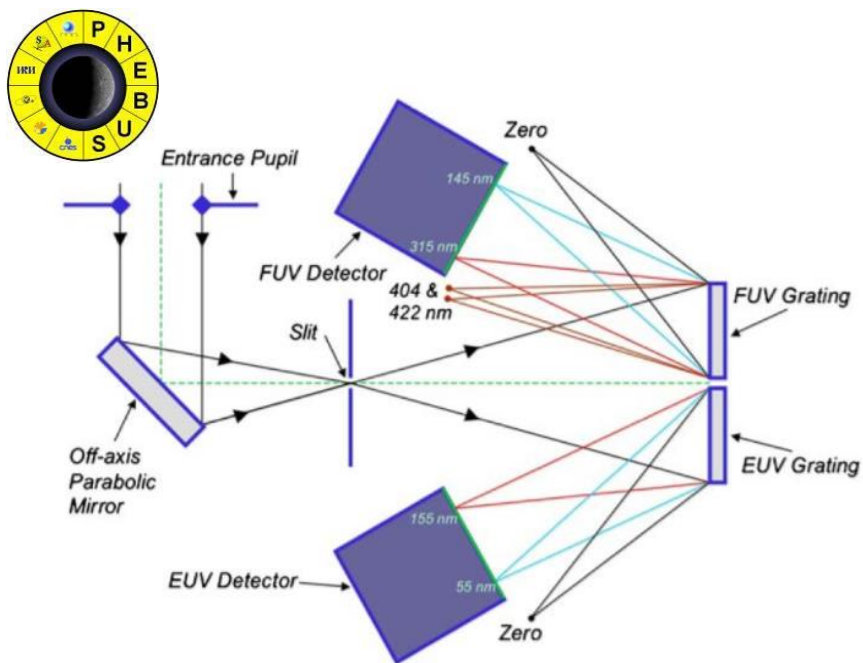
General overview



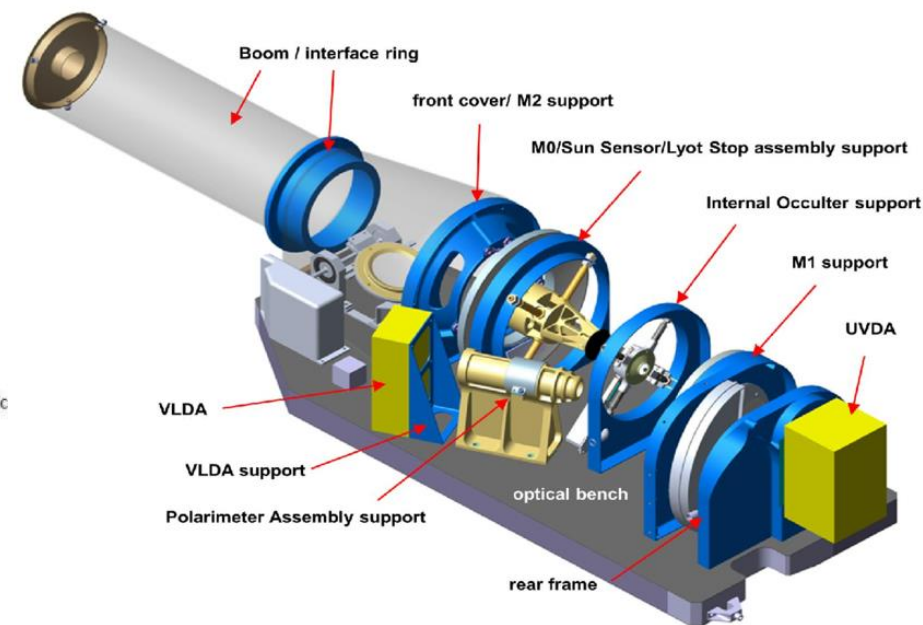
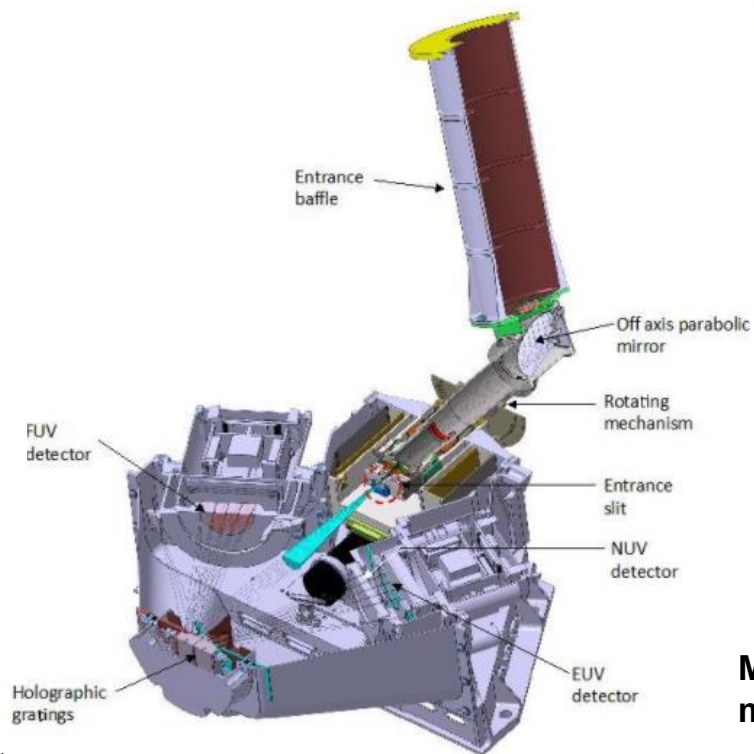
- design, fabrication and testing of optical components for soft x-ray and EUV radiation: mirrors, filters, multilayers



- calibration and characterization of space instruments



PHEBUS–BepiColombo mission
probing of hermean exosphere by ultraviolet spectroscopy



METIS–Solar Orbiter mission
multi element telescope for imaging and spectroscopy

Modeling & Design

SERVER

Rhinoceros
Autocad
Zemax
Shadow
TFCALC
IMD
SRIM/TRIM

Tools for design/optimization of thin film and multilayer structured (home developed)

Samples

DEPOSITION

RF-magnetron sputtering

Electron beam



Characterization

ANALYSIS

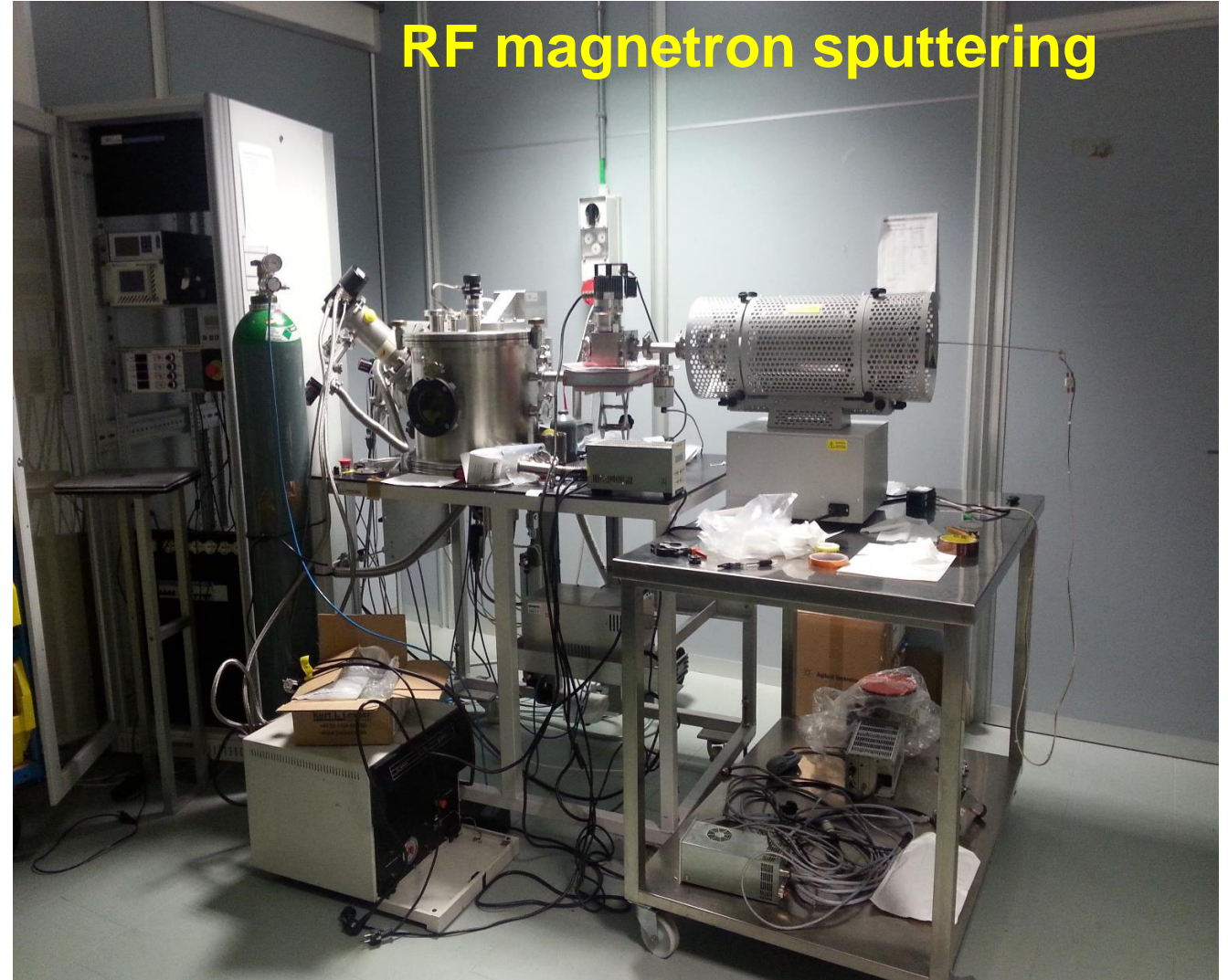
Morphological analysis
Optical Microscope
Profilometer
Atomic Force Microscope (AFM)
Zygo Interferometer

Optical analysis
EUV/VUV McPherson monochromator
ELETTRA Synchrotron
UV/VIS/IR Double Spectrophotometer

e-beam



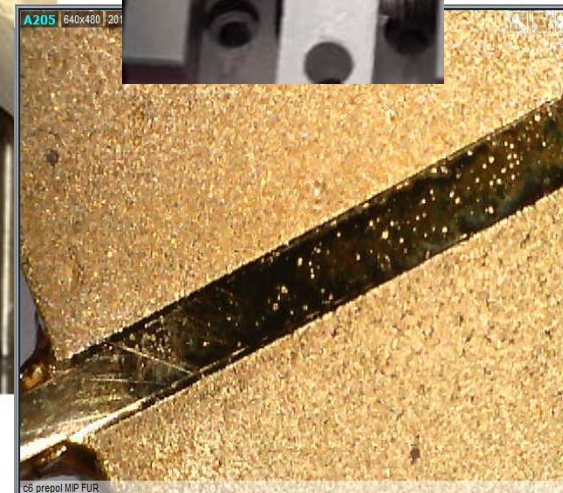
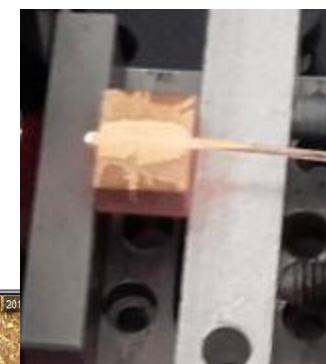
RF magnetron sputtering



Uniformity over 5 cm
Samples up to 20 cm
4 materials
Layer control: 1 nm



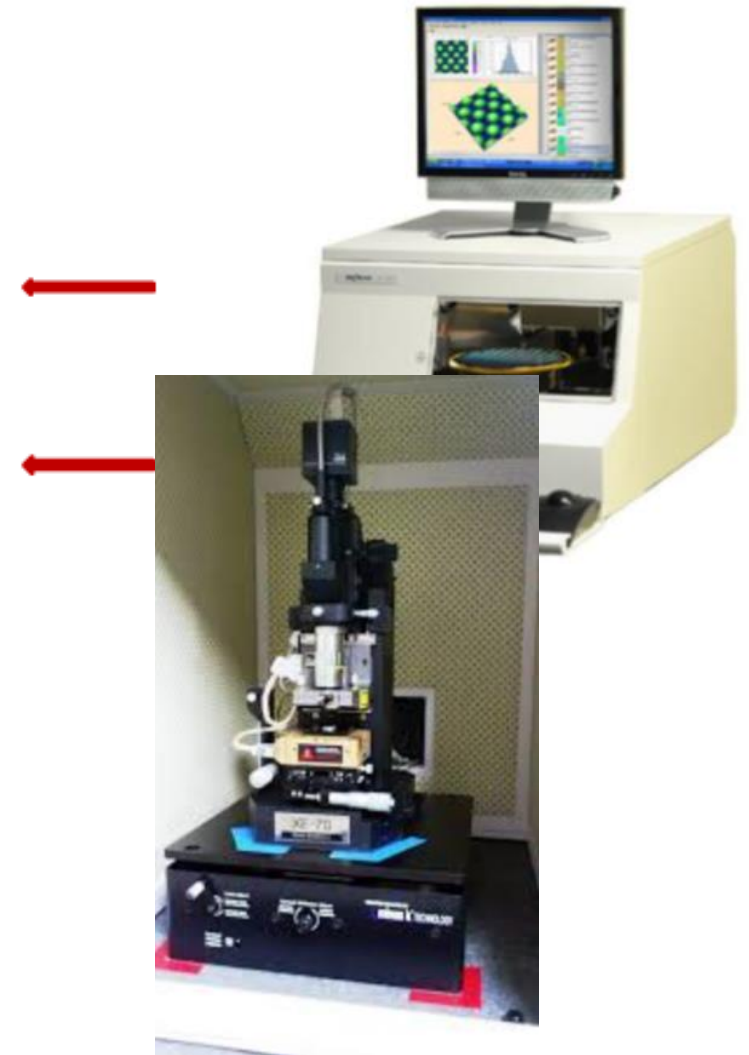
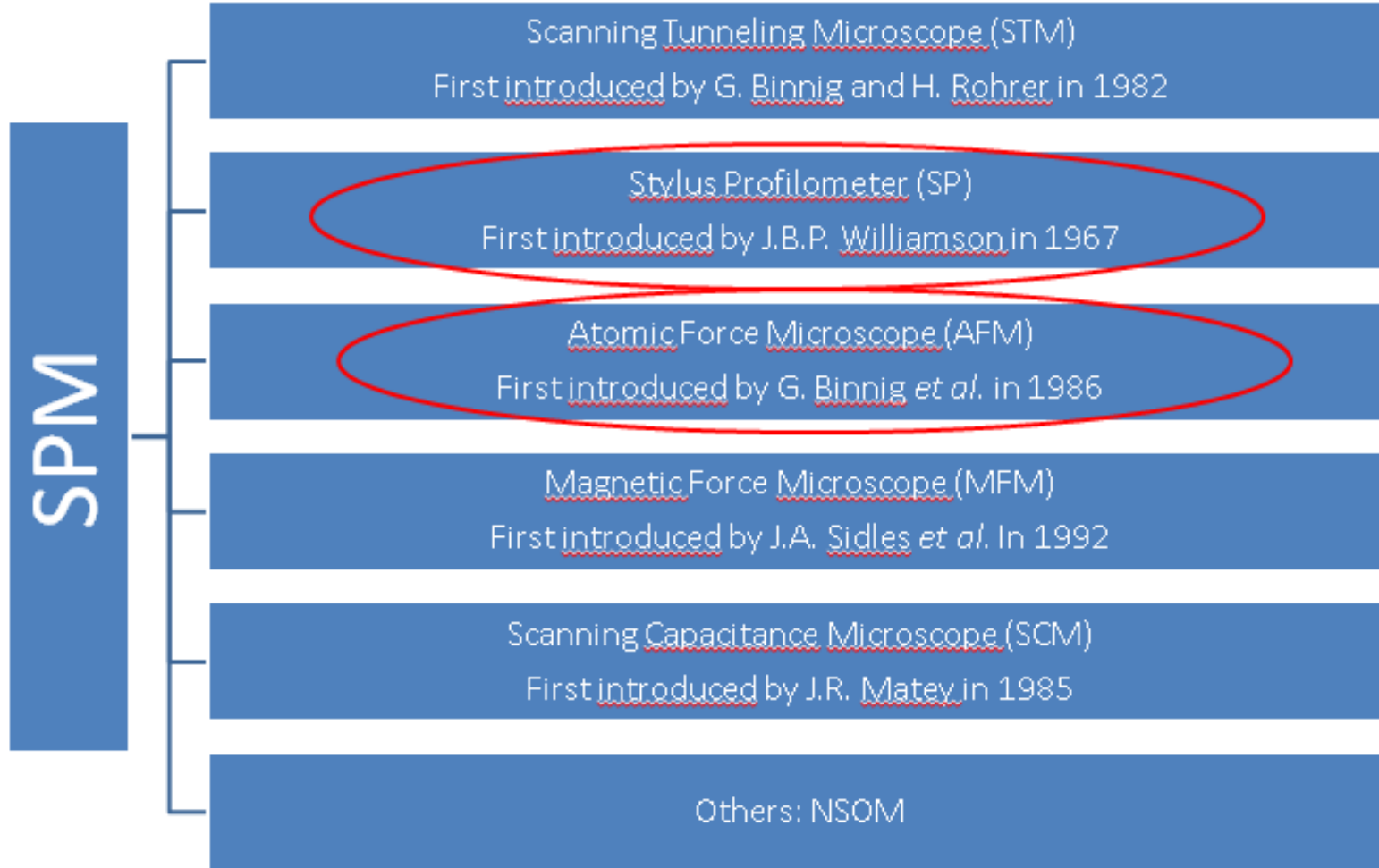
e-beam



Samples up to 1"
2 cathods, 4"
2 calibrated gas lines (O₂, Ar)+ 2 additional lines
Layer control: 0.1 nm

RF magnetron sputtering





Advantages

1. wide range of resolution ($100\mu\text{m}$ - 1\AA)
2. no sample preparation
3. measurement in air, no vacuum
4. wide variety of samples:

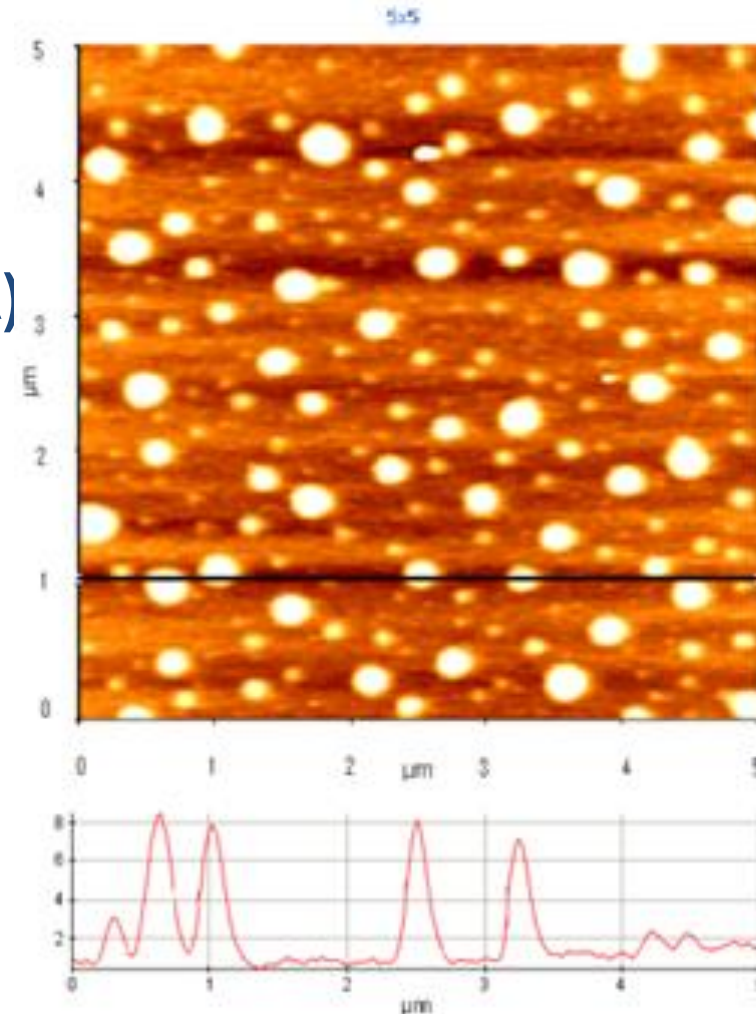
conductor

semiconductor

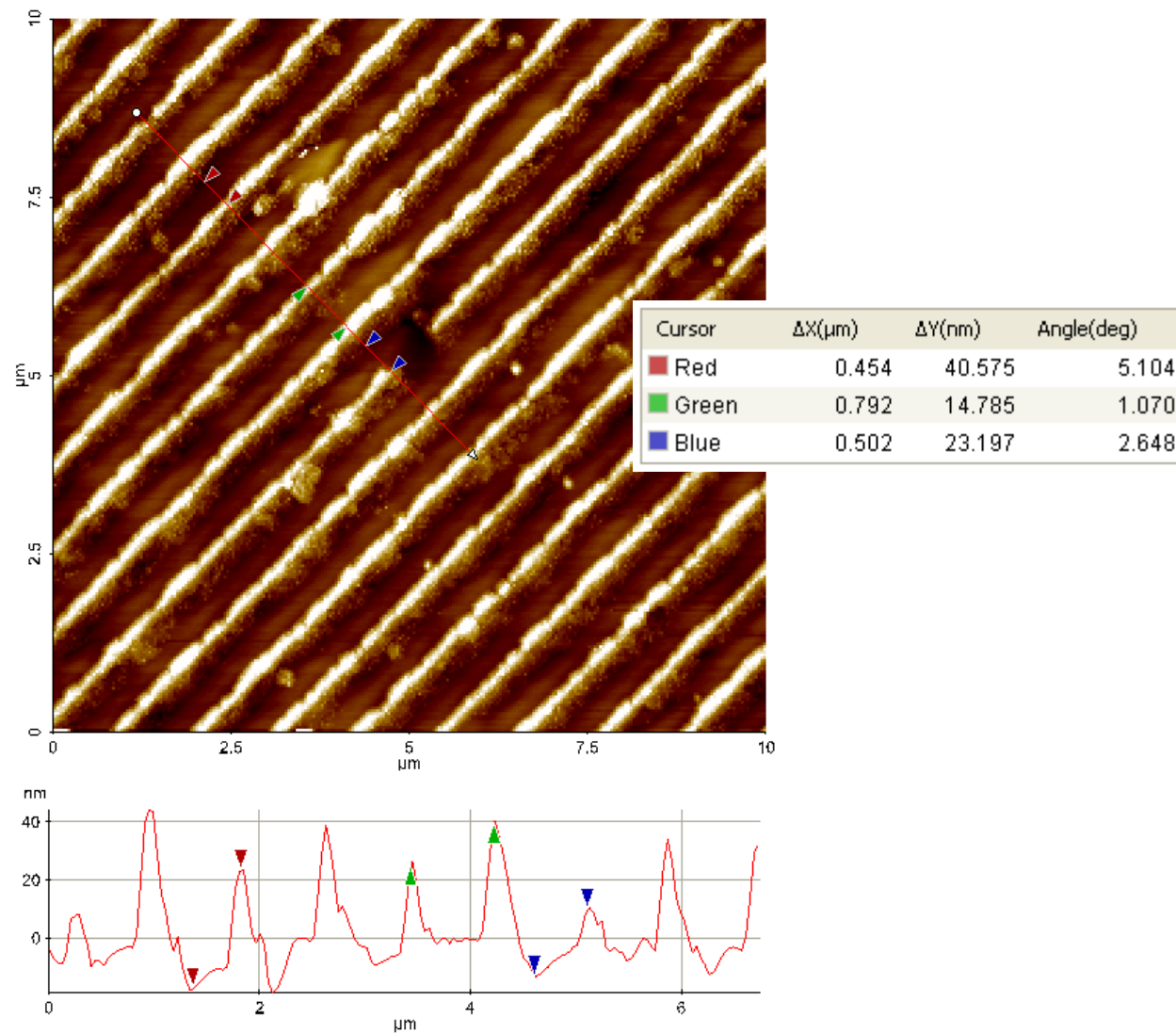
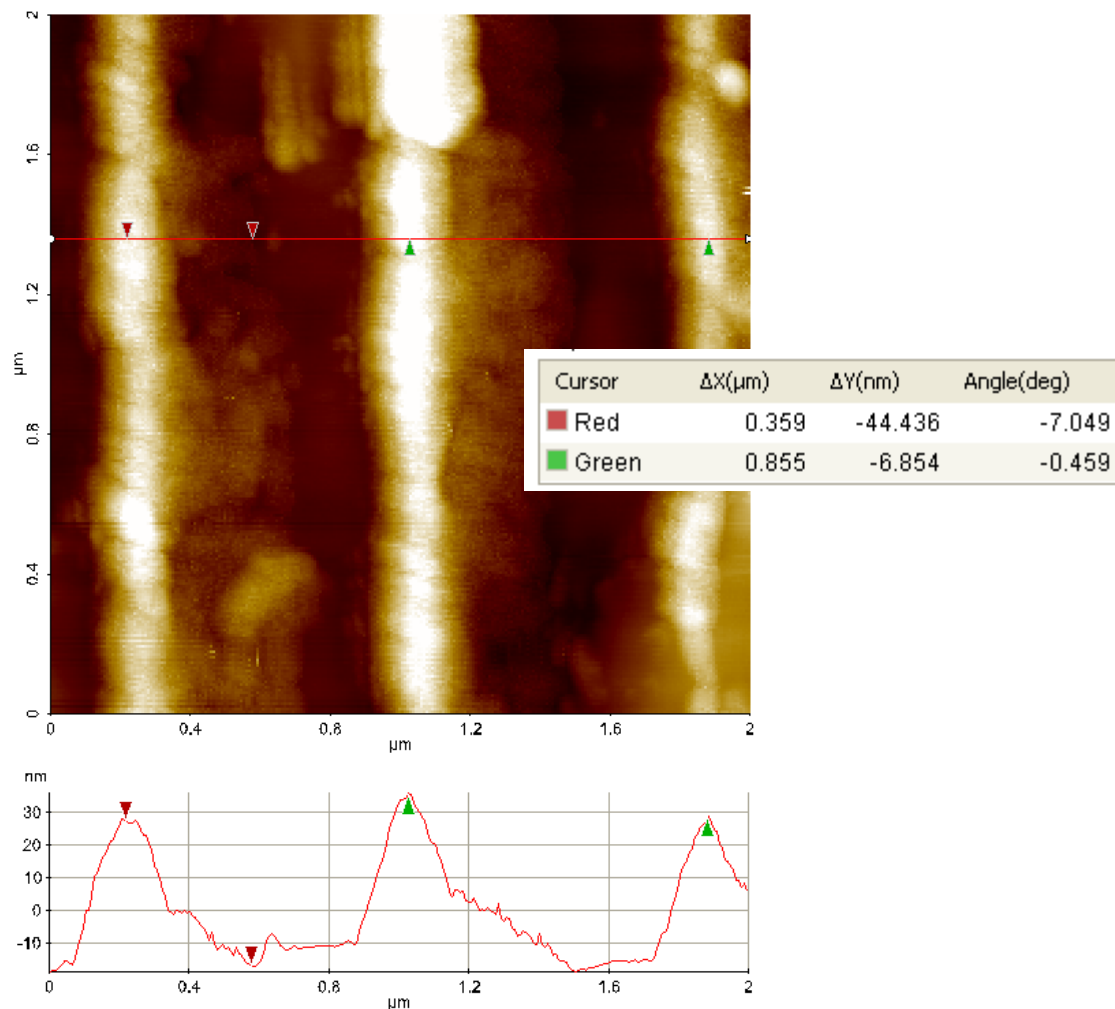
insulator

hard material: oxides, metals

soft materials: wet cells

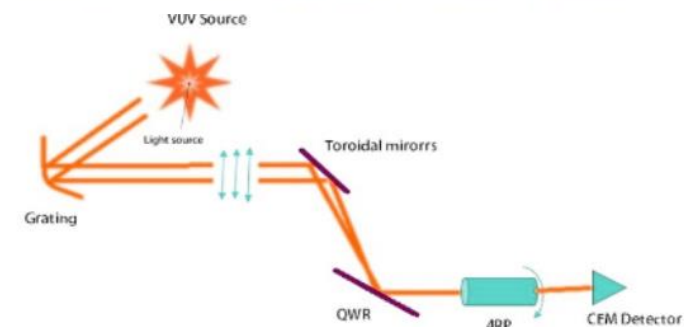
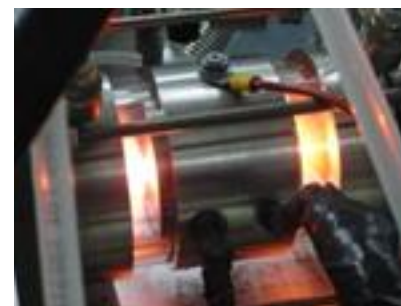
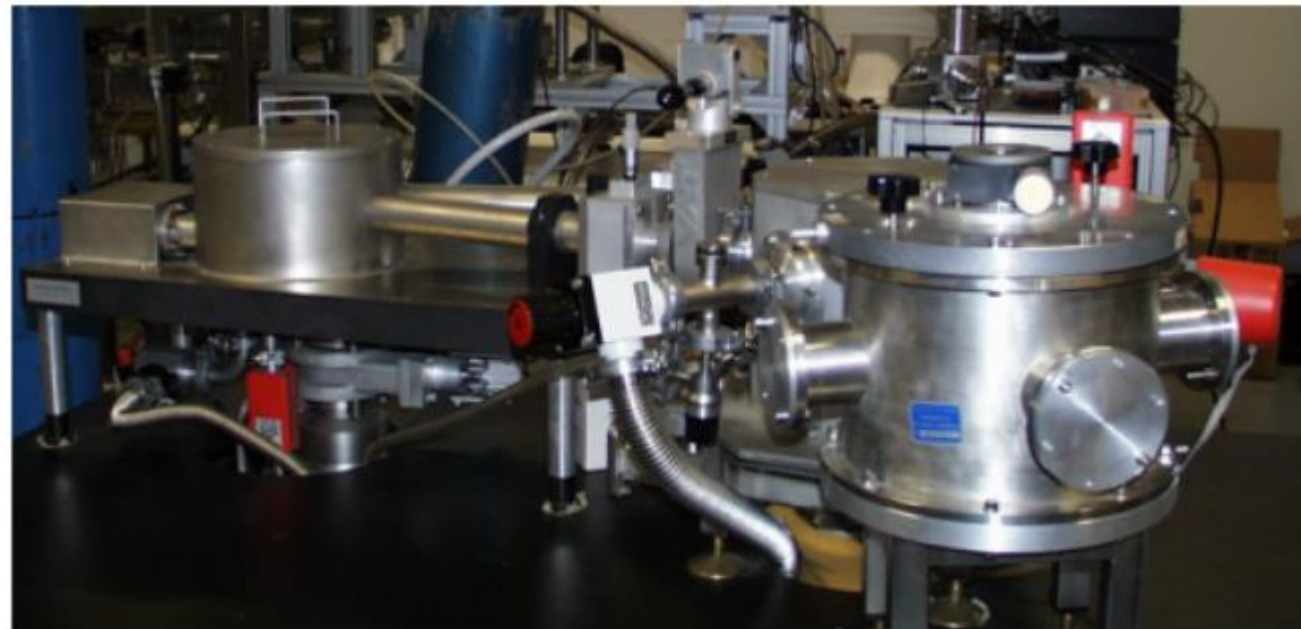
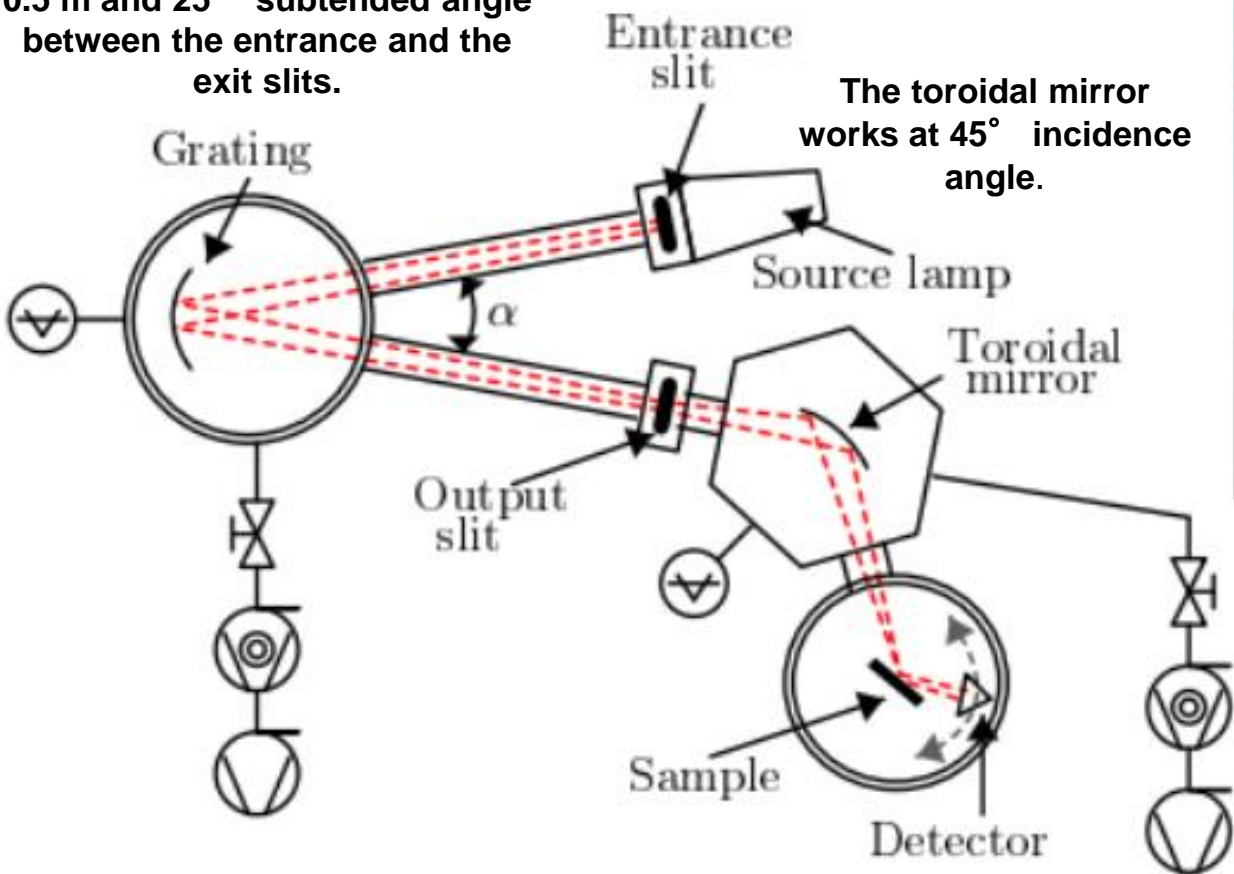


Bubbles induced on Ir/Si multilayers coatings by the exposure to ion bombardments.



AFM topography NO-contact mode Image size 2µmX2µm and 10µmX10µm

600 grooves/mm toroidal Pt-coated grating, main radius of 0.5 m and 25° subtended angle between the entrance and the exit slits.



The samples, and the detector are mounted on movable holders in a θ - 2θ configuration.

Figure. 7. Schematic diagram of the experimental setup. An essentially 90% linearly polarized grating is passed through QWR and analyzed by a Four-reflection polarizer (FRP).

EUV polarimetry in laboratory: thin film characterization and EUV phase retarder reflector development

- Production of linearly and circularly polarized light in vacuum ultraviolet (VUV) and extreme ultraviolet (EUV) spectral ranges has a crucial roles in various science fields such as:
 - Attosecond science
 - Spectroscopic ellipsometry
 - Photolithography
 - Magneto-optical spectroscopy
- Designing a tunable Quarter Wave Retarders works within a wide spectral range (85-160 nm)
- Implementation and characterization of the EUV reflectometer facility for ellipsometry measurements in 85-160 nm spectral range
- Accomplish an alternative tool for fast and preliminary experiments compared to measurements sessions at large scale facilities.
- The system can be a very promising laboratory equipment to characterize phase retarders, polarizers and other optics in the EUV region and to investigate the properties of thin films.

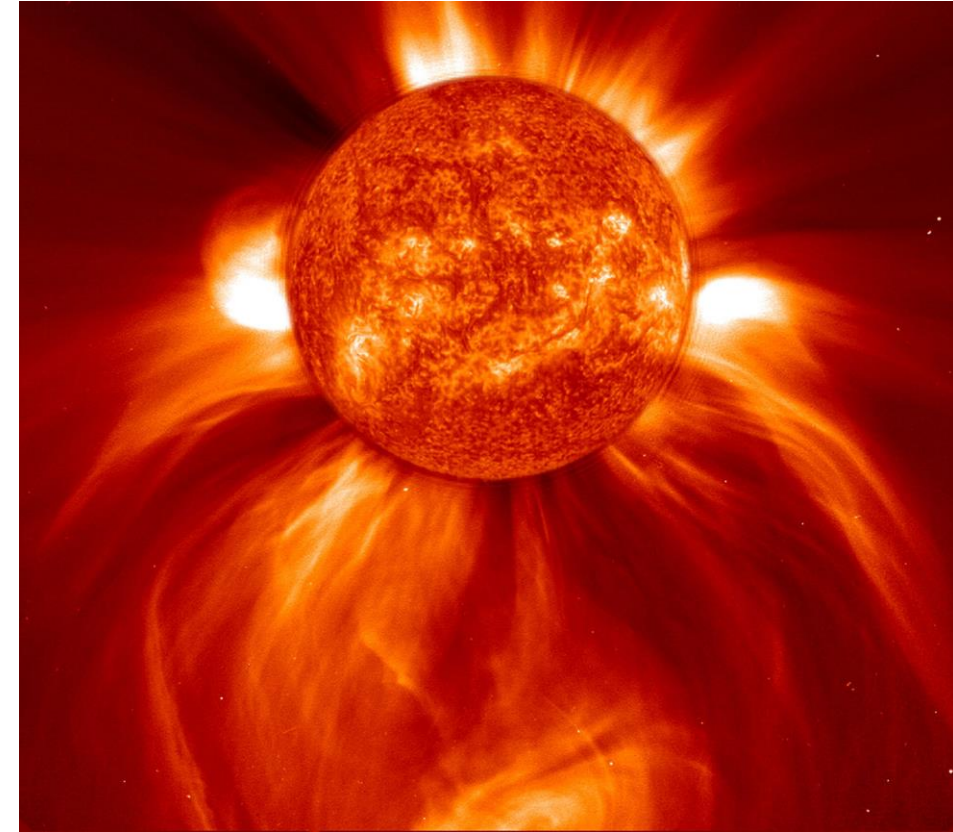
Why polarimetry in the EUV range?

SOLAR PHYSICS

Polarimetry is a powerful tool to interpret how the coronal plasma is involved in the energy transfer processes from the Sun's inner parts to the outer space.

The extreme ultraviolet and the far ultraviolet polarimetry provides essential information of processes governed by the Doppler and Hanle resonant electron scattering effects.

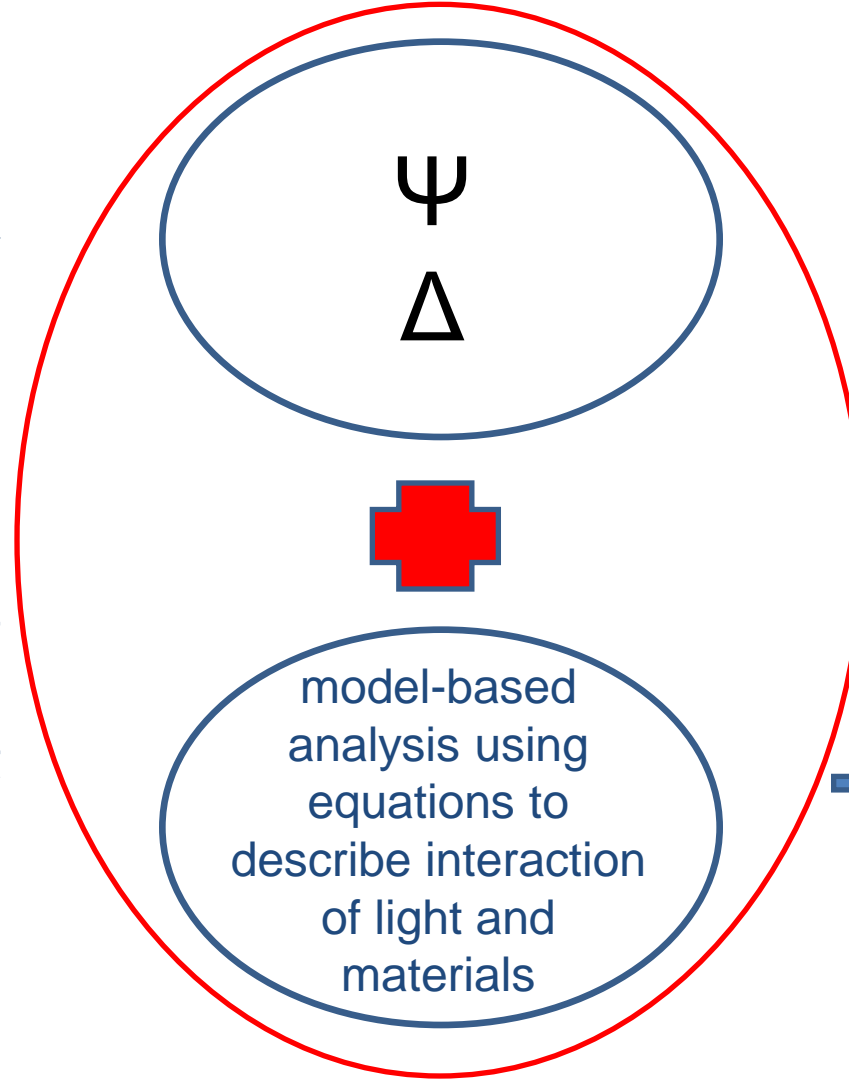
Among the key EUV-FUV spectral lines to observe these processes, H I Lyman α (121.6 nm) is the most intense.



Coronal mass ejections

THIN FILM CHARACTERIZATION

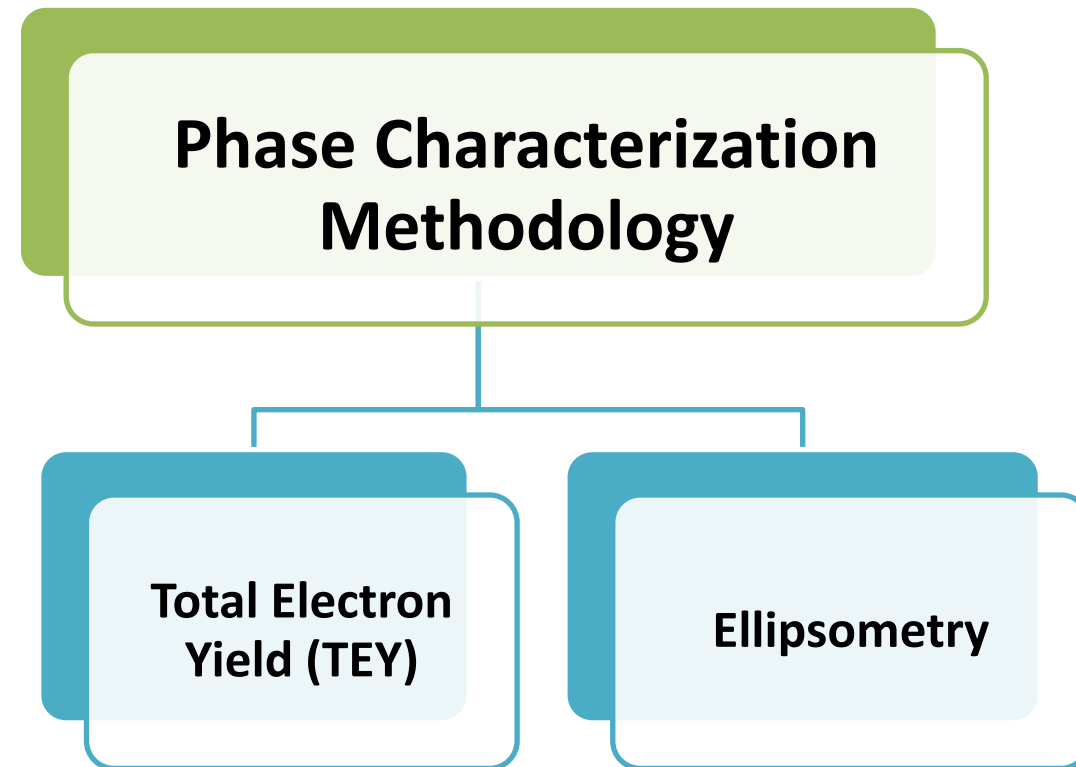
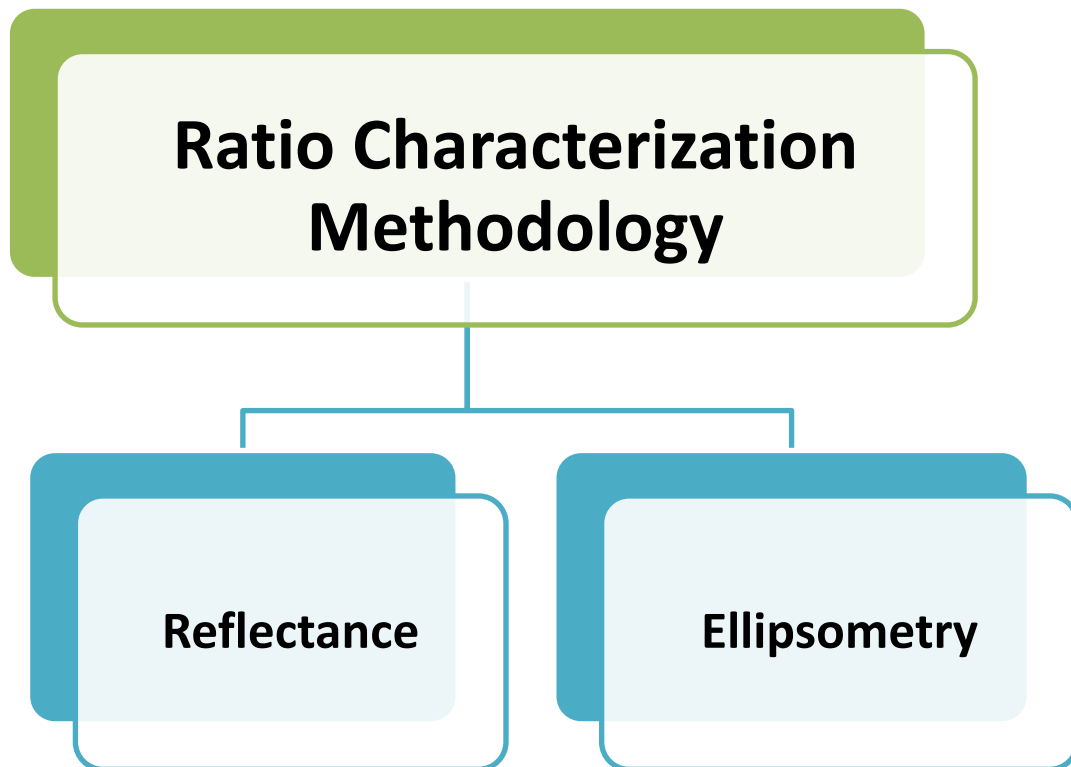
In the materials science, ellipsometry is considered one of the promising and superior technique for revealing the optical and structural properties of materials, since linearly and circularly polarized radiations are very sensitive to the interaction of light with electrons of materials and compounds. The method is not invasive and can give information about the sample with high-precision.

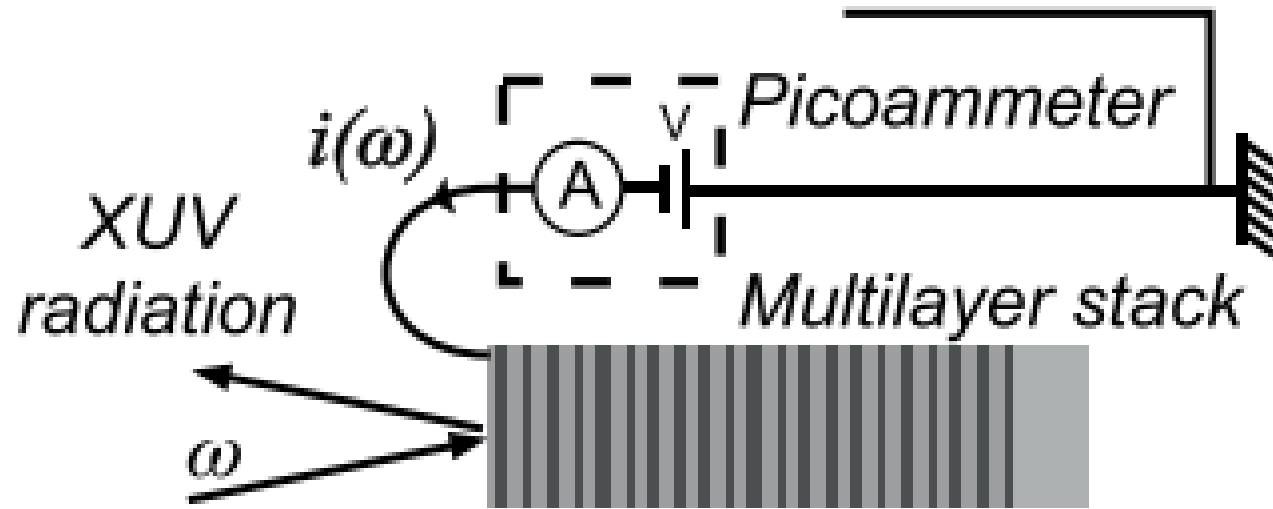


The measured values are expressed as ψ and Δ . These values are related to the ratio of Fresnel reflection coefficients r_p and r_s for -p and -s polarized light.

$$\rho = \frac{r_p}{r_s} = \tan(\psi) e^{i\Delta}$$

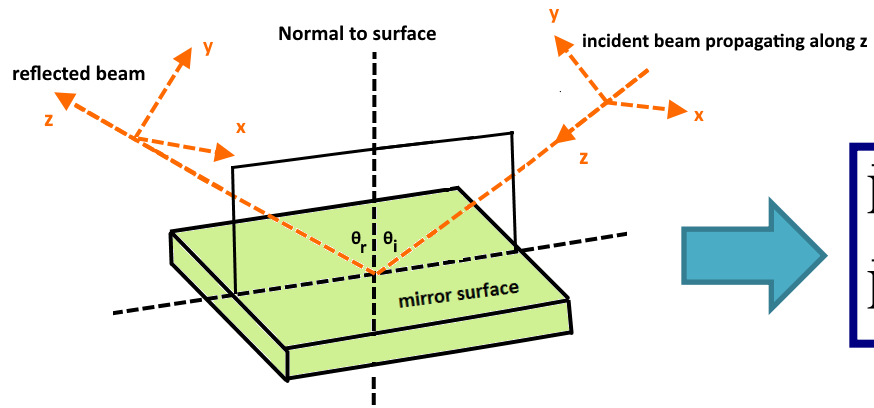
- film thickness
- refractive index
- surface roughness
- interface regions
- composition
- crystallinity
- anisotropy
- uniformity





$$\text{TEY}(E) = C(E)I_0(E) \left(1 + R(E) + 2\sqrt{R(E)} \cos \phi(E) \right)$$

$C(E)$ is a constant of the sample, $I_0(E)$ is the linearly-polarized incident beam irradiance, $R(E)$ is the reflectance of the sample in s-polarization and $\phi(E)$ is the phase delay induced upon reflection.



$$\vec{E}_x(z,t) = E_{0x} \cos(kz - \omega t) \vec{x}$$

$$\vec{E}_y(z,t) = E_{0y} \cos(kz - \omega t + \varepsilon) \vec{y}$$

Stokes parameters

$$S_0 = I = E_{0x}^2 + E_{0y}^2$$

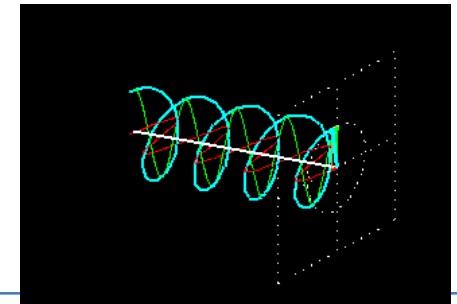
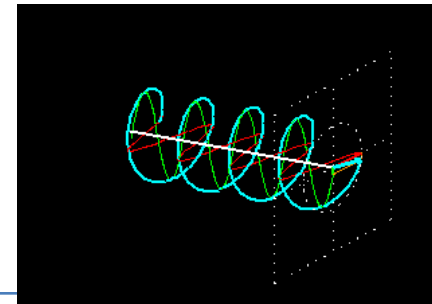
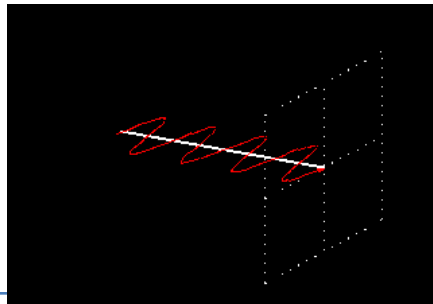
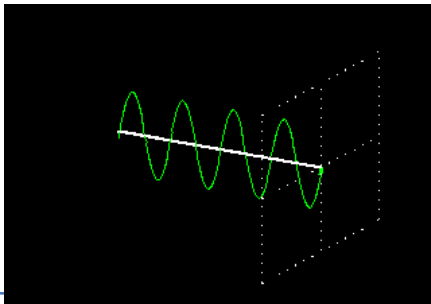
$$S_1 = Q = E_{0x}^2 - E_{0y}^2$$

$$S_2 = U = 2E_{0x}E_{0y} \cos \varepsilon$$

$$S_3 = V = 2E_{0x}E_{0y} \sin \varepsilon$$

The reference system used in the experiment. Incident linearly polarized light with electric field vector E_i propagates along the z axis, suitably chosen values of the incident angle θ_i and rotation angle θ

The polarization state of a light beam is described by the Stokes parameters. In the reference system defined in the figure, the electric vector E of monochromatic electromagnetic wave travels along the z-axis. In the general case, we can decompose the vector into E_{0x} and E_{0y} components, respectively along the x and y directions. The Stokes parameters characterize the light beam in terms of intensities and phase difference ε . S_0 is the total irradiance of the light beam, the parameter S_1 describes the amount of horizontal or vertical linear polarization, the parameter S_2 describes the amount of $+45^\circ$ or -45° linear polarization, while the parameter S_3 describes the amount of right or left circular polarization, and $\varepsilon = \varepsilon_y - \varepsilon_x$ is the phase difference between the two components.



The polarization ellipse is only valid at a given instant of time (function of time):

$$\left(\frac{E_x(t)}{E_{0x}(t)} \right)^2 + \left(\frac{E_y(t)}{E_{0y}(t)} \right)^2 - 2 \frac{E_x(t)}{E_{0x}(t)} \frac{E_y(t)}{E_{0y}(t)} \cos \varepsilon = \sin^2 \varepsilon$$

To get the Stokes parameters, do a time average (integral over time) and a little bit of algebra...

$$\left(E_{0x}^2 + E_{0y}^2 \right)^2 - \left(E_{0x}^2 - E_{0y}^2 \right)^2 - \left(2E_{0x}E_{0y} \cos \varepsilon \right)^2 = \left(2E_{0x}E_{0y} \sin \varepsilon \right)^2$$

$$S_0 = I = E_{0x}^2 + E_{0y}^2$$

$$S_1 = Q = E_{0x}^2 - E_{0y}^2$$

$$S_2 = U = 2E_{0x}E_{0y}\cos \varepsilon$$

$$S_3 = V = 2E_{0x}E_{0y}\sin \varepsilon$$

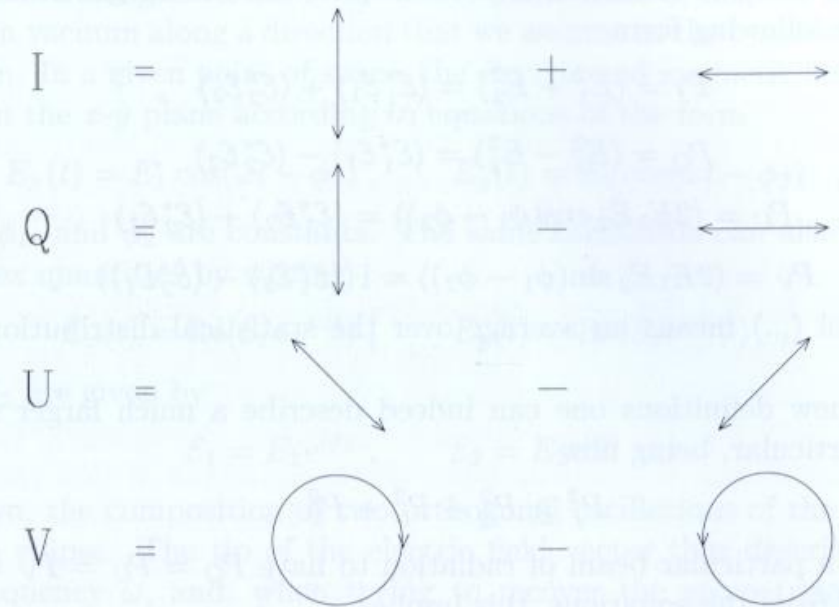


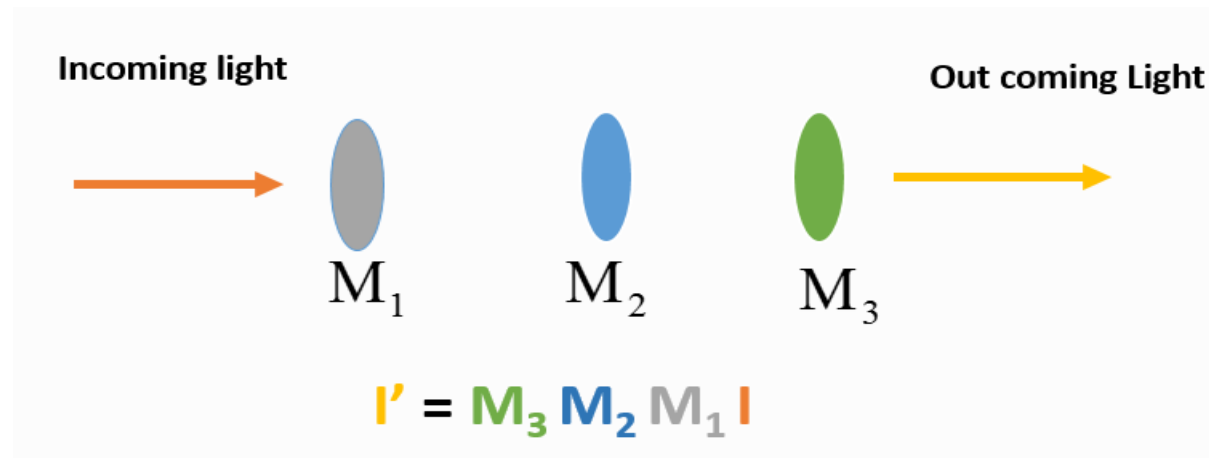
FIGURE 1. Pictorial representation of the Stokes parameters. The observer is supposed to face the radiation source.

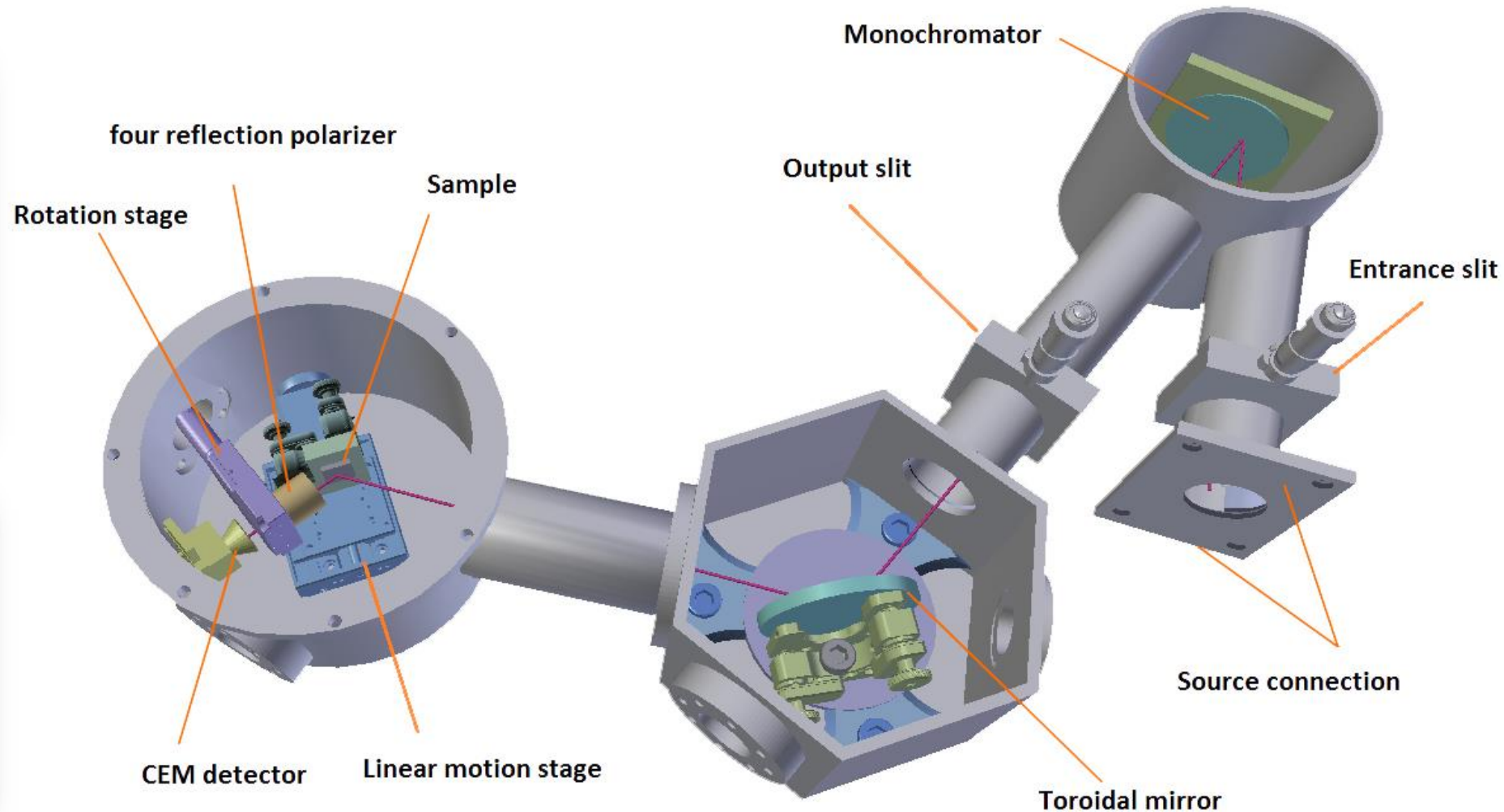
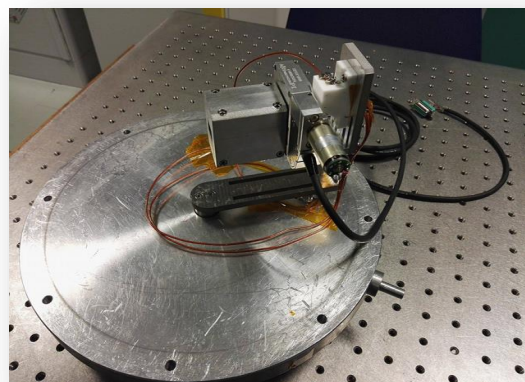
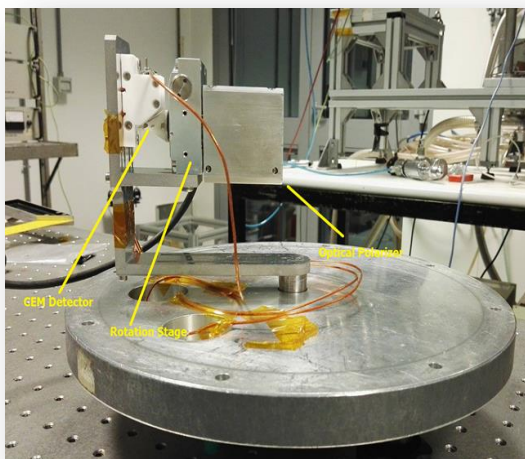
When the beam goes through an optical element its polarization changes, then the Stokes parameters change. The effect of the optical element is described by the related Mueller matrix M . M is 4×4 matrix.

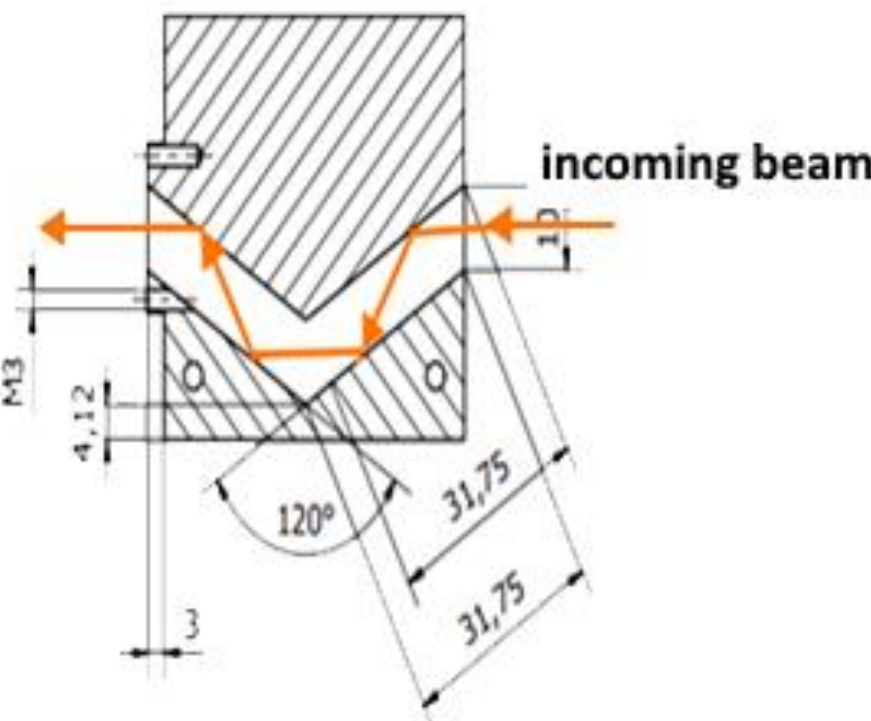
$$S' = \mathcal{M} \cdot S$$

$$\begin{bmatrix} S'_0 \\ S'_1 \\ S'_2 \\ S'_3 \end{bmatrix} = \begin{bmatrix} M_{00} & M_{01} & M_{02} & M_{03} \\ M_{10} & M_{11} & M_{12} & M_{13} \\ M_{20} & M_{21} & M_{22} & M_{23} \\ M_{30} & M_{31} & M_{32} & M_{33} \end{bmatrix} \begin{bmatrix} S_0 \\ S_1 \\ S_2 \\ S_3 \end{bmatrix}$$

The concept of the Mueller calculus can be extended to complex optical equipment, composed by a set of elements; the equivalent Mueller matrix of the whole system is given by the product of the Mueller matrix of each element..

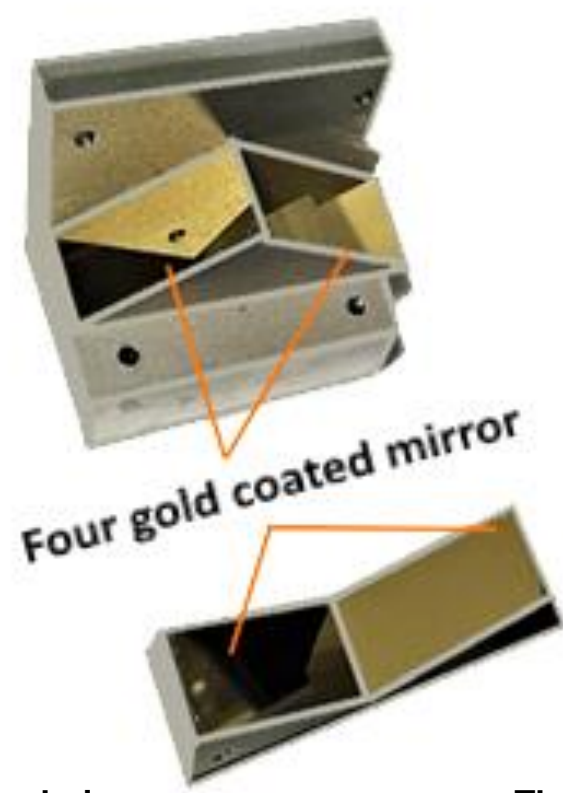






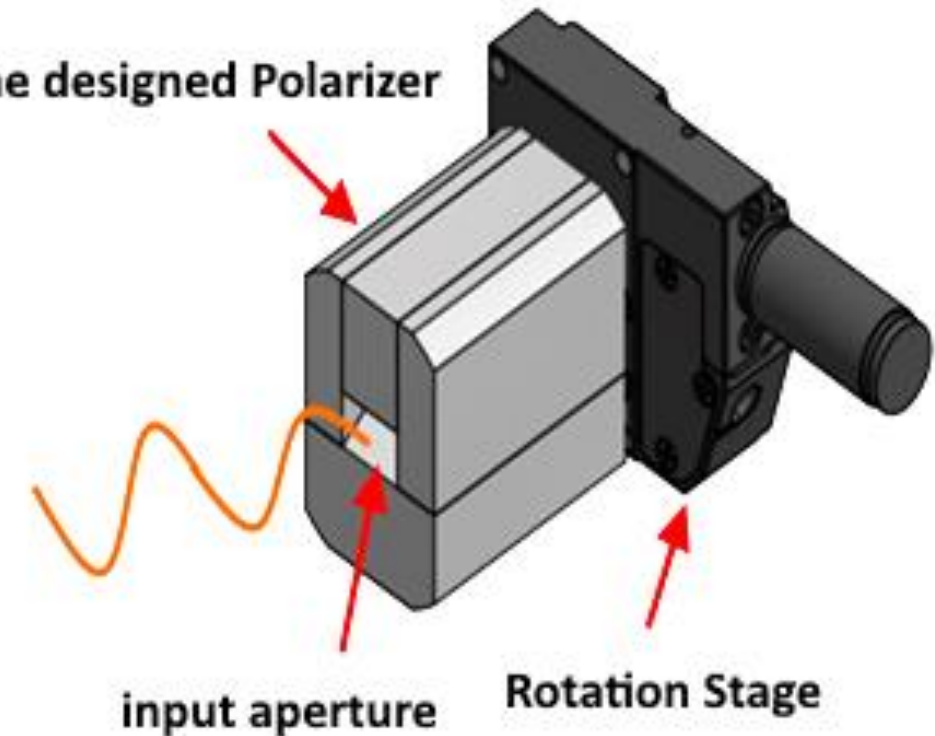
(a)

It is a four-reflection linear polarizer optimized for the H-Lyman alpha line and fabricated by using gold coated mirrors consisting of 200 nm thick films deposited by thermal evaporation on Si substrate.



(b)

The designed Polarizer

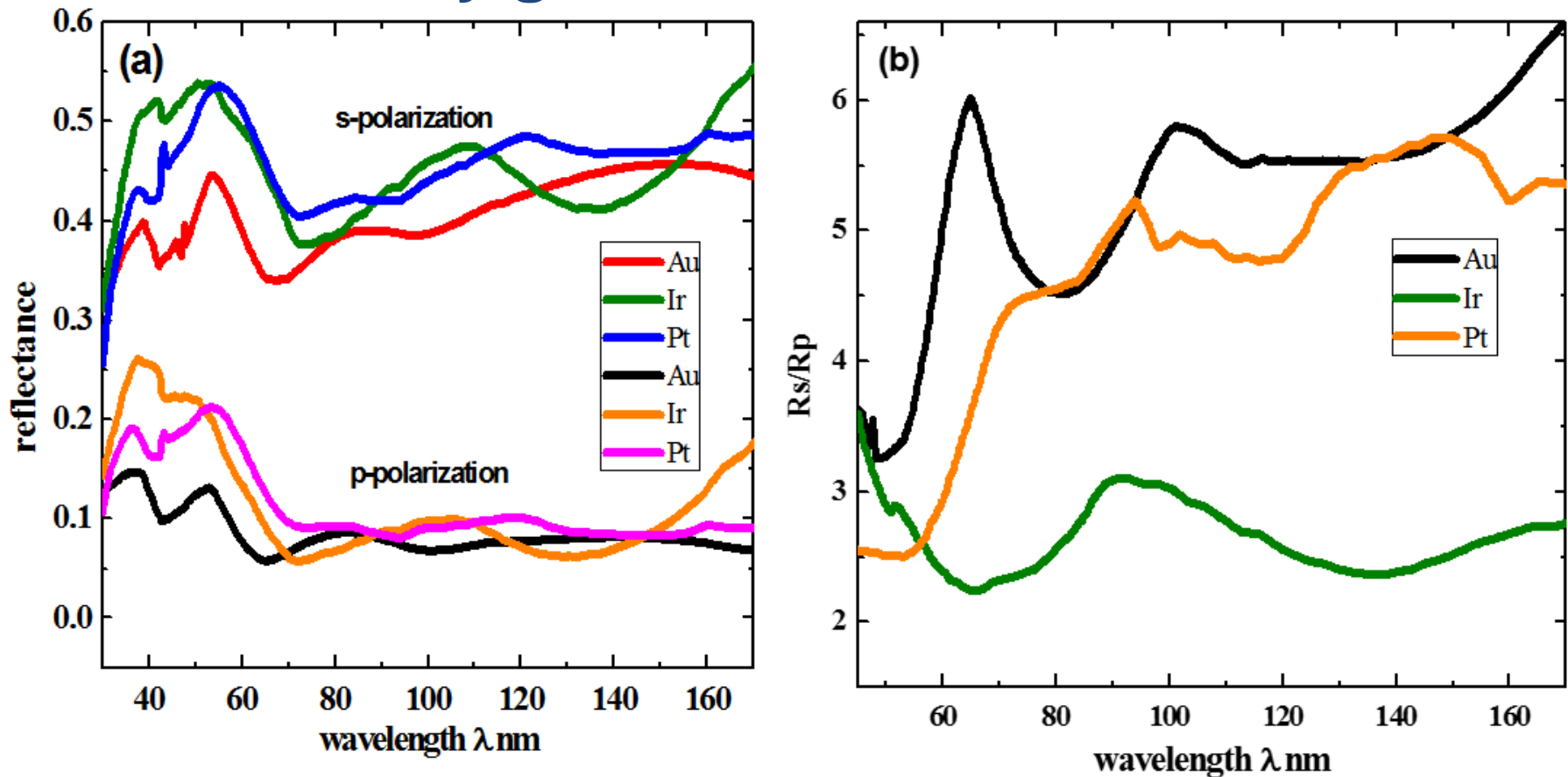


(c)

The design guarantees that the performances of the polarizer are relatively good even on an extended spectral range from 40 nm to 160 nm.

Why gold?

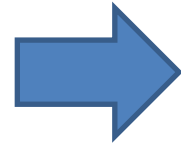
Gold is a good reflector in the 40–160 nm range, it is very stable and the optical constants are well known. However, a single gold surface at the Brewster angle is not enough for reaching high extinction coefficient.^c



Calculated reflectance R_s and R_p versus wavelengths at normal incidence angle of 60° ; (b) ratio $\frac{R_s}{R_p}$ of Au, Ir, and Pt coatings on Si substrate for different wavelengths.

In case of the four-reflection linear polarizer used in the experiment, the net Müller matrix is:

$$M_{FRP} = M.M.M.M = (M)^4$$



$$M_{FRP} = \begin{bmatrix} \frac{|r_s|^8 + |r_p|^8}{2} & \frac{|r_s|^8 + |r_p|^8}{2} & 0 & 0 \\ \frac{|r_s|^8 + |r_p|^8}{2} & \frac{|r_s|^8 + |r_p|^8}{2} & 0 & 0 \\ 0 & 0 & r_s^4 r_p^4 & 0 \\ 0 & 0 & 0 & r_s^4 r_p^4 \end{bmatrix}$$

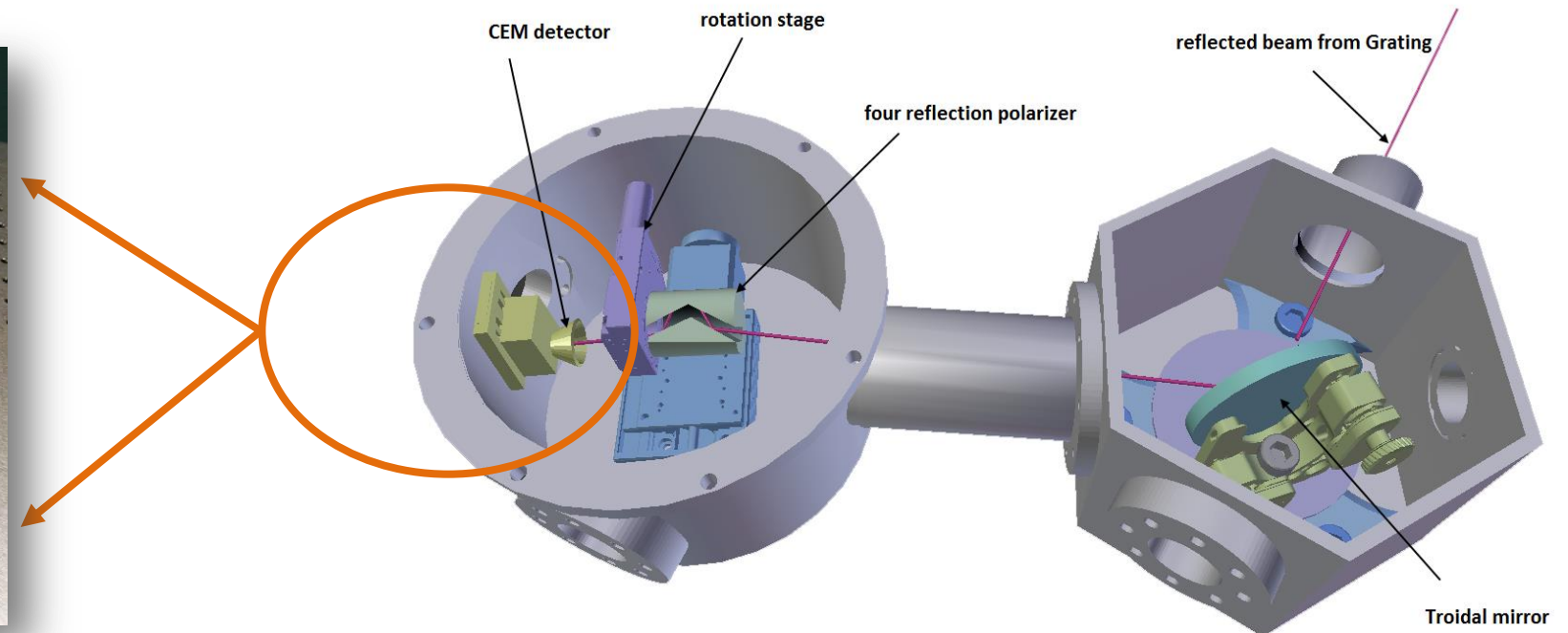
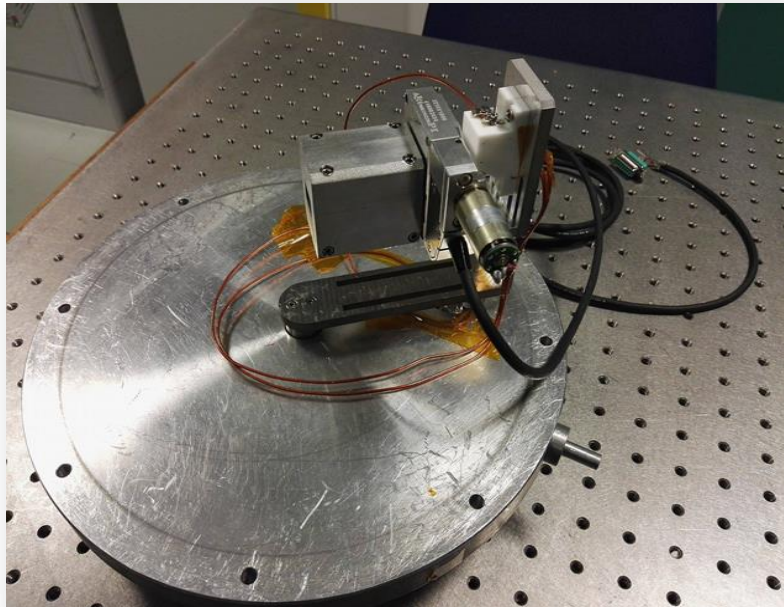
The polarizer can rotate around its axis, then a Mueller matrix for a rotator is needed and the mathematical representation of rotated polarizer is expressed by the following relationship

$$R(-\theta).M_{FRP}.R(\theta)$$

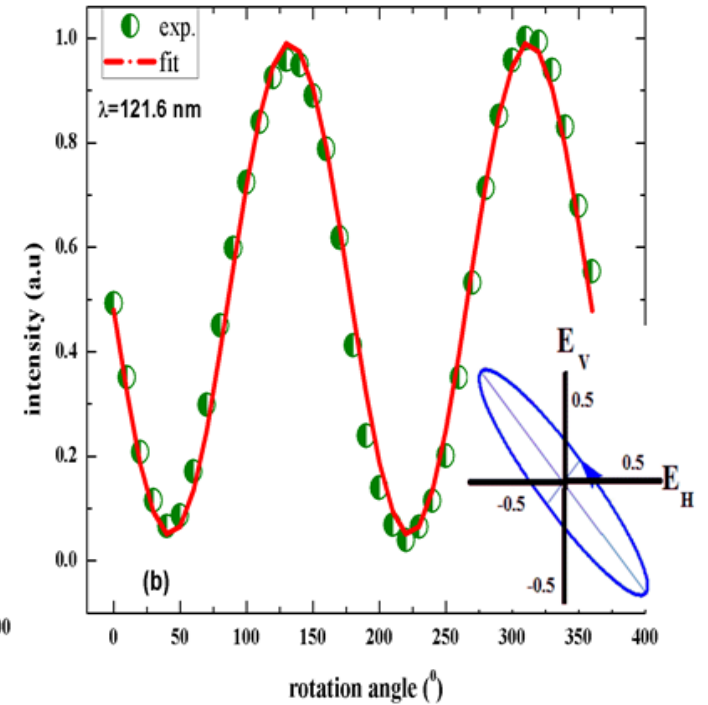
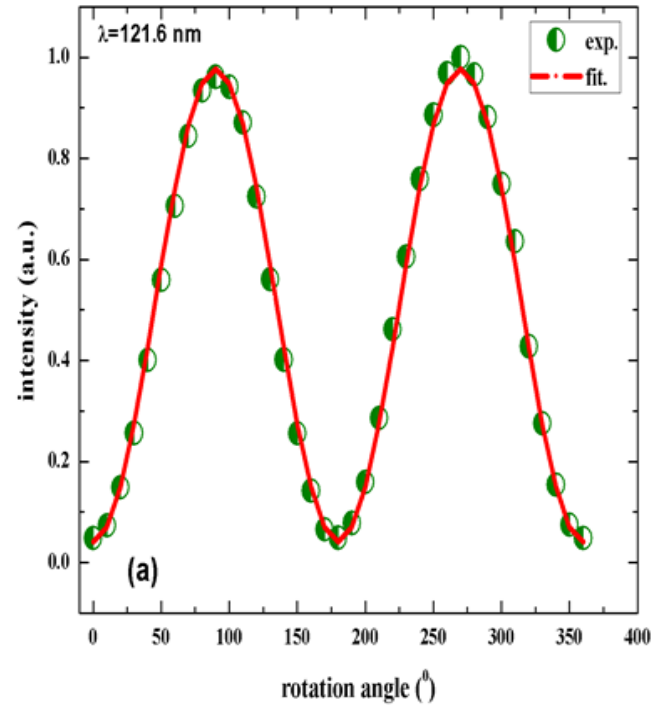
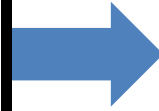
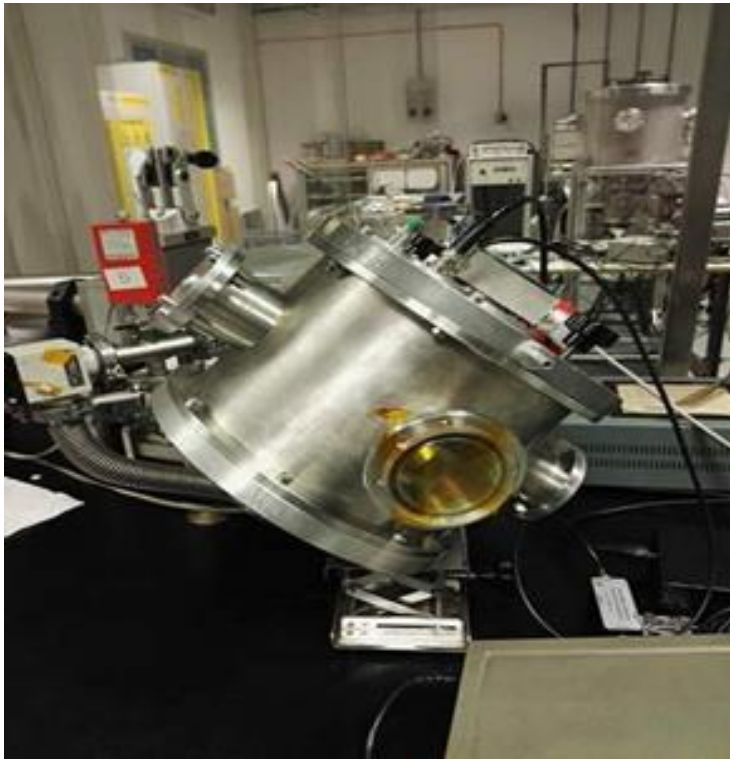
$$\begin{pmatrix} \frac{|r_s|^8 + |r_p|^8}{2} & \frac{|r_s|^8 - |r_p|^8}{2} \cos 2\theta & \frac{|r_s|^8 - |r_p|^8}{2} \sin 2\theta & 0 \\ \frac{|r_s|^8 - |r_p|^8}{2} \cos 2\theta & \frac{|r_s|^8 + |r_p|^8}{2} \cos^2 2\theta + r_s^4 r_p^4 \sin^2 2\theta & \frac{|r_s|^8 + |r_p|^8}{2} \cos 2\theta \sin 2\theta - r_s^4 r_p^4 \sin^2 2\theta \cos 2\theta & 0 \\ \frac{|r_s|^8 - |r_p|^8}{2} \sin 2\theta & \frac{|r_s|^8 + |r_p|^8}{2} \sin 2\theta \cos 2\theta - r_s^4 r_p^4 \cos 2\theta \sin 2\theta & \frac{|r_s|^8 + |r_p|^8}{2} \sin^2 2\theta + r_s^4 r_p^4 \cos^2 2\theta & 0 \\ 0 & 0 & 0 & r_s^4 r_p^4 \end{pmatrix}$$

The beam is allowed to pass through the Four-reflection polarizer (FRP) rotated clockwise with respect to the beam propagation direction around the beam axis by an angle (θ), the equivalent Mueller matrix of the system is defined as

$$S_0^{\sim} = \frac{1}{2} \left((|r_s|^8 + |r_p|^8) S_0 + (|r_s|^8 - |r_p|^8) S_1 \cos 2\theta + (|r_s|^8 - |r_p|^8) S_2 \sin 2\theta \right)$$



Schematic diagram of the experimental apparatus for the polarization measurements at EUV reflectometer.



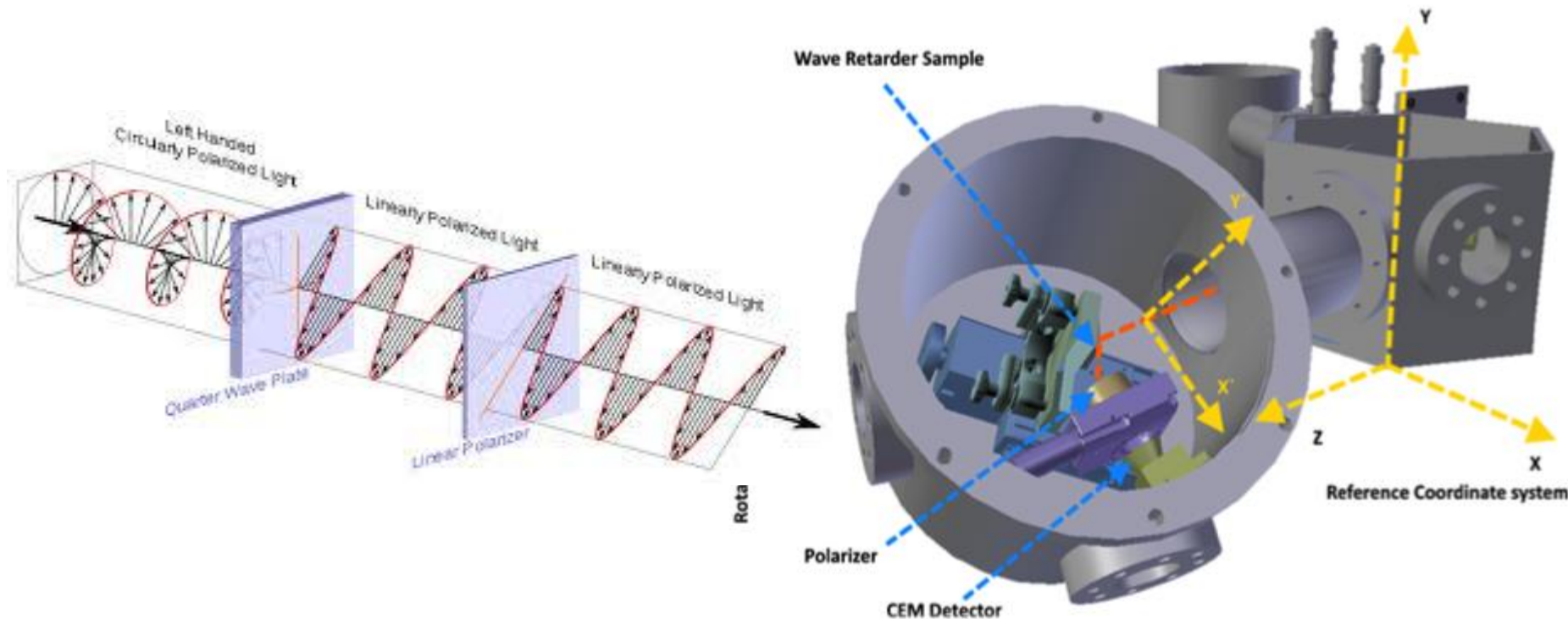
$$S_0 \sim \frac{1}{2} \left((|r_s|^8 + |r_p|^8) S_0 + (|r_s|^8 - |r_p|^8) S_1 \cos 2\theta + (|r_s|^8 - |r_p|^8) S_2 \sin 2\theta \right)$$



- a) almost fully polarized light along the y axis. (Fig. a);
- b) almost fully -45° polarized light as described by the polarization ellipse (Fig. b).

Stokes Vector	a) almost fully polarized light along the y axis	b) almost fully -45° polarized light
S ₀	1	1
S ₁	-0.92	-0.006
S ₂	-0.002	-0.90

In order to determine the fourth Stokes parameter, an optical element acting on the polarization state of the beam must be introduced along the optical path. We select an aluminum coating and we characterize both the beam and the phase retarder. The optical scheme is shown in the figure. The beam reflected by the phase retarder element was analyzed by the polarizer and recorded by the CEM detector.



Experimental Setup for testing the QWR in the FUV-EUV facility at Padova.

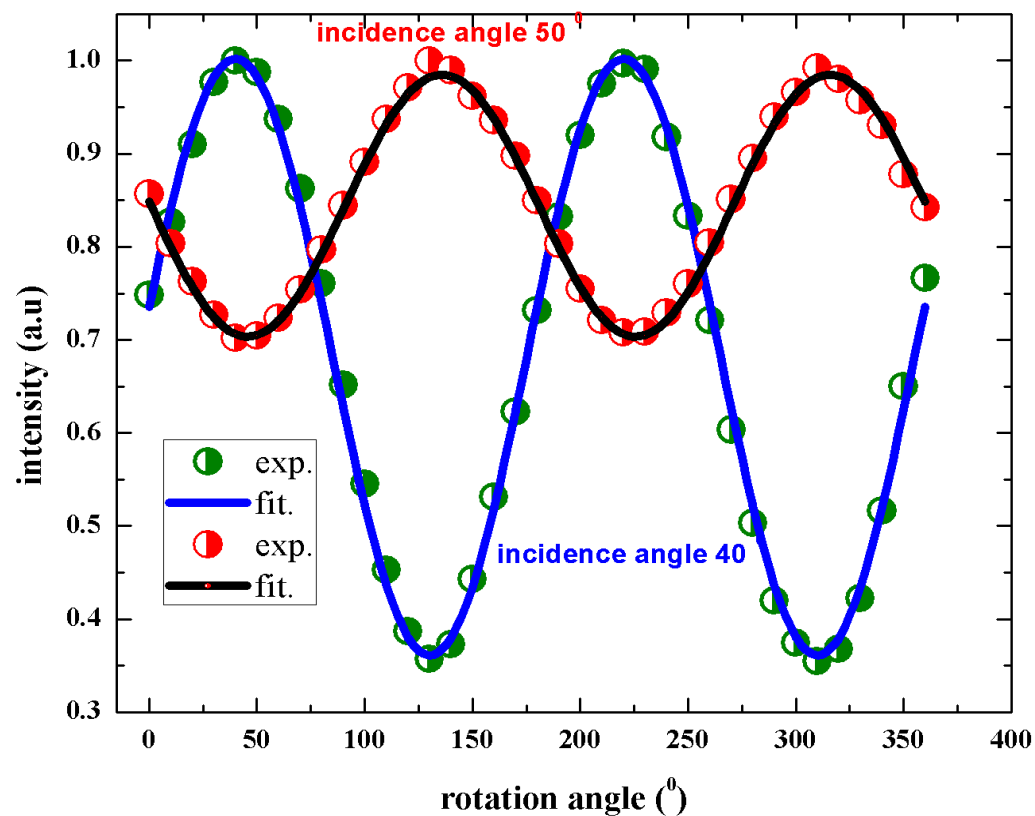
3D design of the set up arrangement for testing the QWRs, the testing chamber rotated by 45°

$$S = R(-\theta)M(FRP)R(\theta)M(R)S_0$$

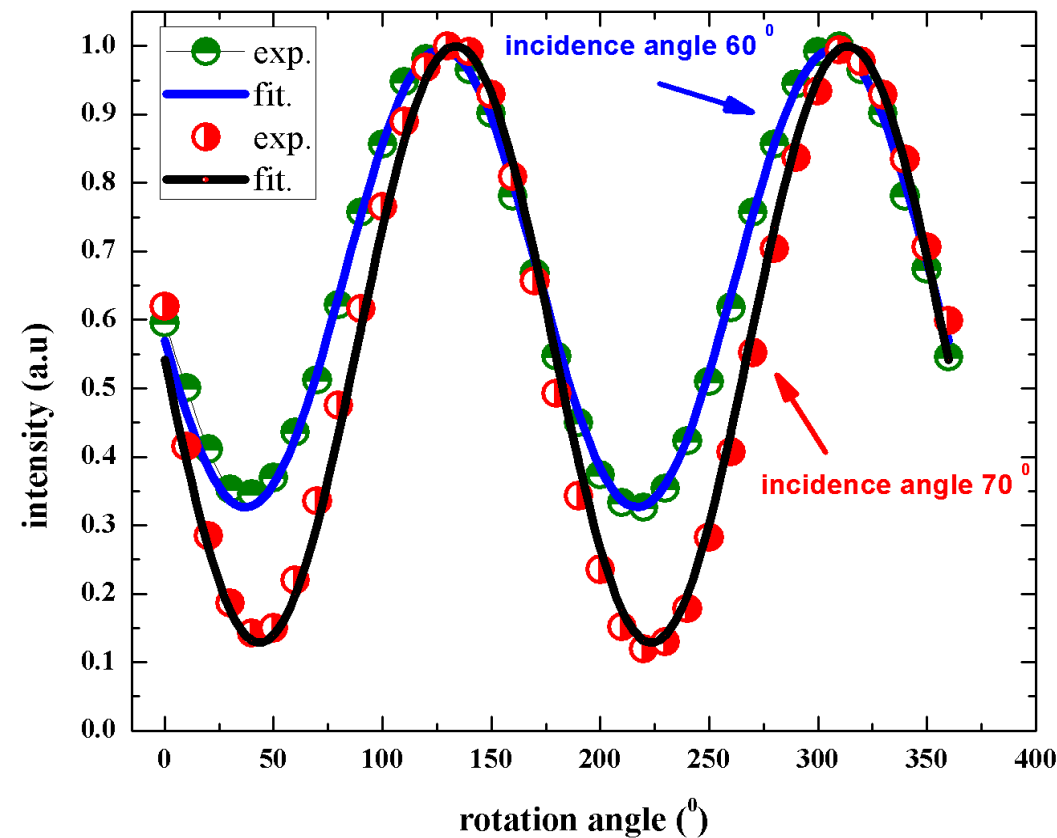
$$M_{\text{Retarder}} = \begin{pmatrix} \frac{|r_s^R|^2 + |r_p^R|^2}{2} & \frac{|r_s^R|^2 - |r_p^R|^2}{2} & 0 & 0 \\ \frac{|r_s^R|^2 - |r_p^R|^2}{2} & \frac{|r_s^R|^2 + |r_p^R|^2}{2} & 0 & 0 \\ 0 & 0 & |r_s^R||r_p^R|\cos\delta & |r_s^R||r_p^R|\sin\delta \\ 0 & 0 & -|r_s^R||r_p^R|\sin\delta & |r_s^R||r_p^R|\cos\delta \end{pmatrix}$$

The detected intensity is:

$$S_0^{\sim} = \frac{1}{4} \left(\begin{aligned} & \left((|r_s|^8 + |r_p|^8) \cdot (|r_{sR}|^2 + |r_{pR}|^2) + (|r_s|^8 - |r_p|^8) \cdot (|r_{sR}|^2 - |r_{pR}|^2) \cdot \cos 2\theta \right) \cdot S_0 \\ & + \left((|r_s|^8 + |r_p|^8) \cdot (|r_{sR}|^2 - |r_{pR}|^2) + (|r_s|^8 - |r_p|^8) \cdot (|r_{sR}|^2 + |r_{pR}|^2) \cdot \cos 2\theta \right) \cdot S_1 \\ & + (|r_s|^8 - |r_p|^8) r_s^R r_p^R \cdot \cos \delta \cdot \sin 2\theta \cdot S_2 \\ & + (|r_s|^8 - |r_p|^8) r_s^R r_p^R \cdot \sin \delta \cdot \sin 2\theta \cdot S_3 \end{aligned} \right)$$



Measured and fitted data of aluminum samples at two different incidence angles 40° and 50°



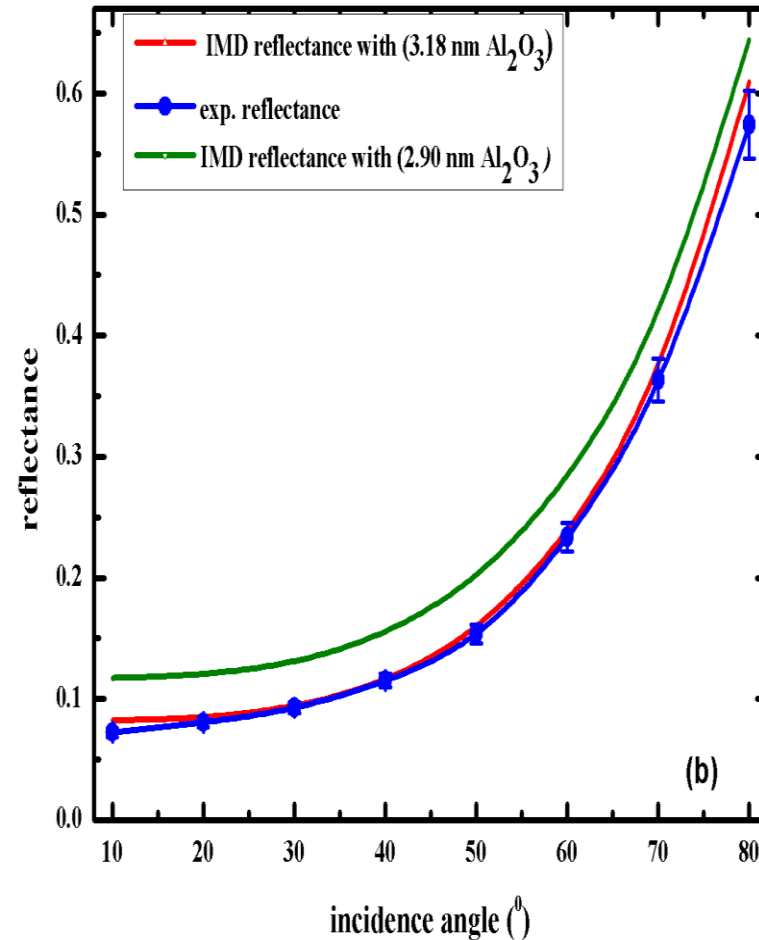
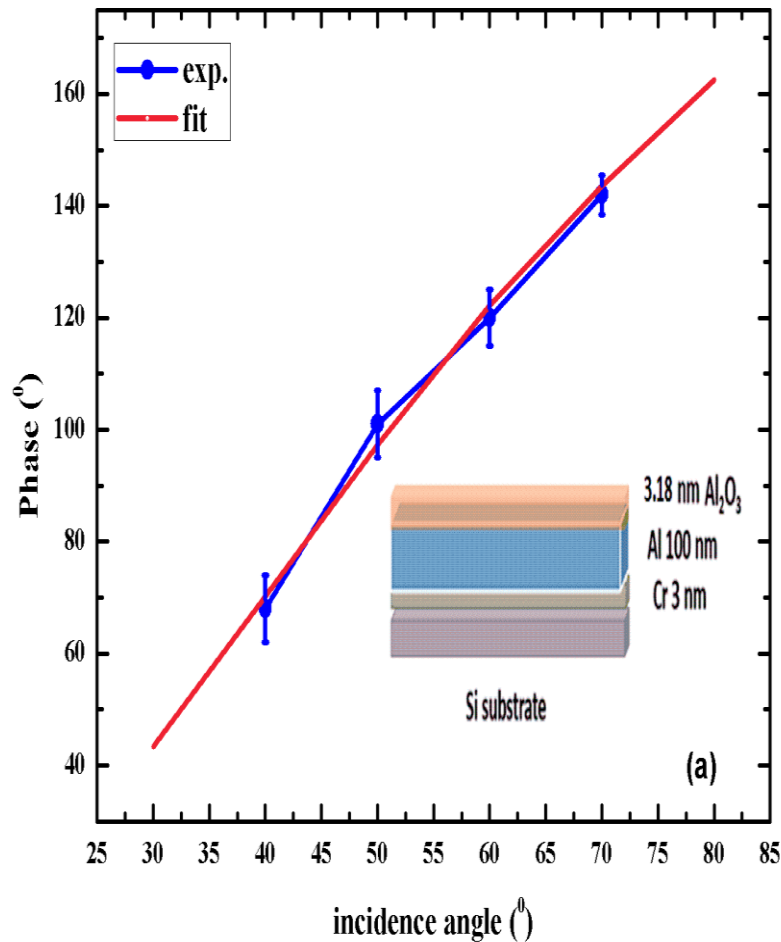
Measured and fitted curves of aluminum samples at two different incidence angles 60° and 70°

QWP ←

Incidence angle	ratio	Δ	STDV Δ	S_3
40	1.12	68	6	0.02
50	1.08	101	6	0
60	0.94	120	6	-0.03
70	1.04	142	5	-0.08

→ Very small!!!

The fitted values of ratio, phase and S_3



The ellipsometric parameters of the sample can be determined quite accurately. The uncertainty associated to the phase is 3% - 9% depending on the incidence angles. The ratio can be derived by measuring the reflectance, the error is derived by the experimental one. We use the phase derived by the ellipsometric measurements in order to retrieve the properties of the sample under investigation and to evaluate the potential of the method and the experimental system capabilities. Aluminum is well known to have a thin oxide layer on its surface due to the reaction with air which strongly affects the optical properties of the film. We fitted the phase experimental data by using IMD software in order to retrieve the thickness of the oxide layer. We used the optical constants of Palik for both Al and Al₂O₃.

The figure show the 'measured' phase versus the incidence angle at wavelength 121.6 nm and the fitted curve by IMD, the determined structure is in the inset. The thickness of the oxide layer determined by the fitting procedure is 3.18 nm ($\chi^2=0.29$).

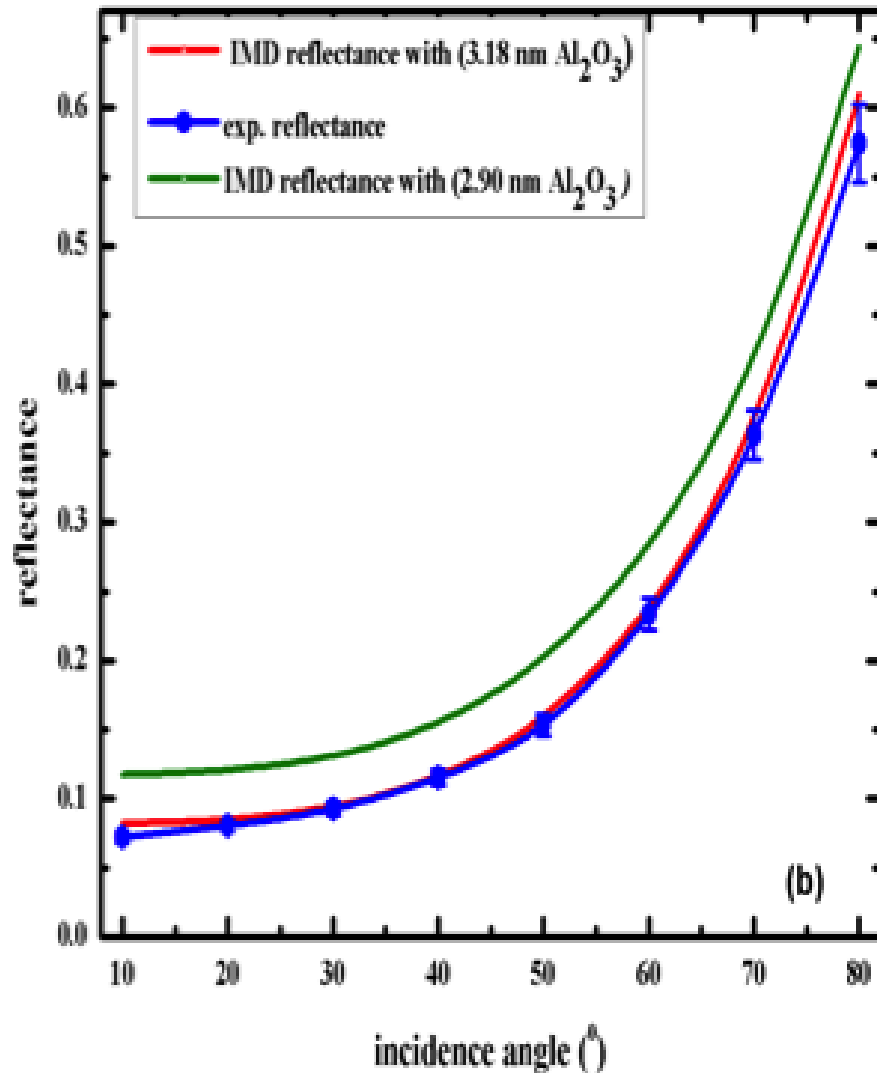
Incidence angle
(°)

Fit (we used the phase) by
IMD software
thickness of the oxide 3.18
nm

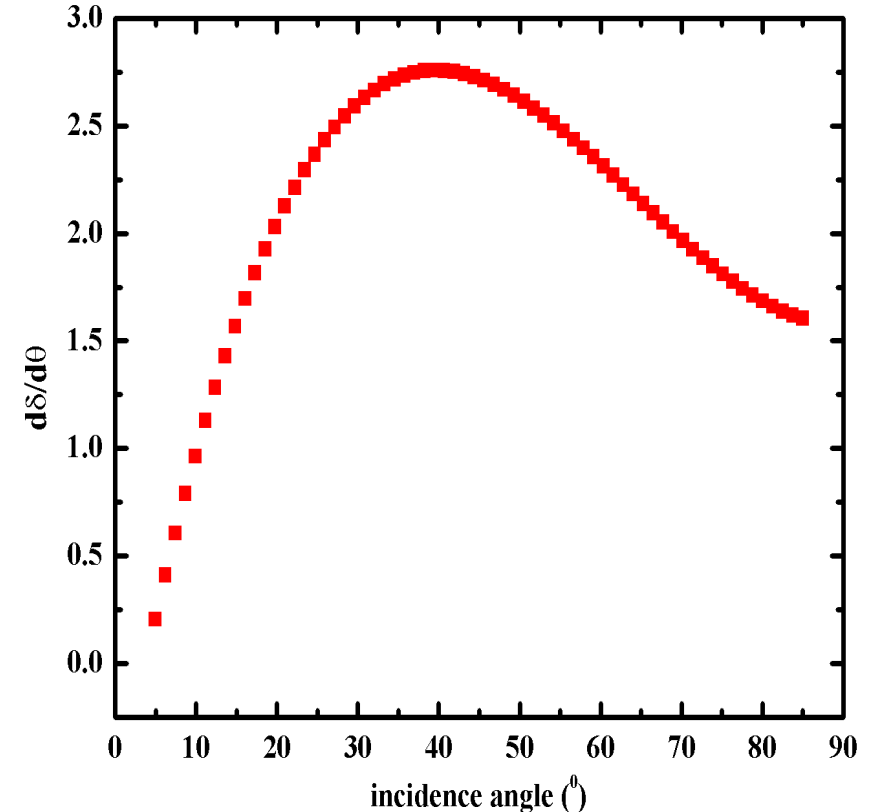
Simulation by IMD software
thickness of the oxide 2.90
nm

Fit by using ellipsometry
measurements (MATLAB
code)

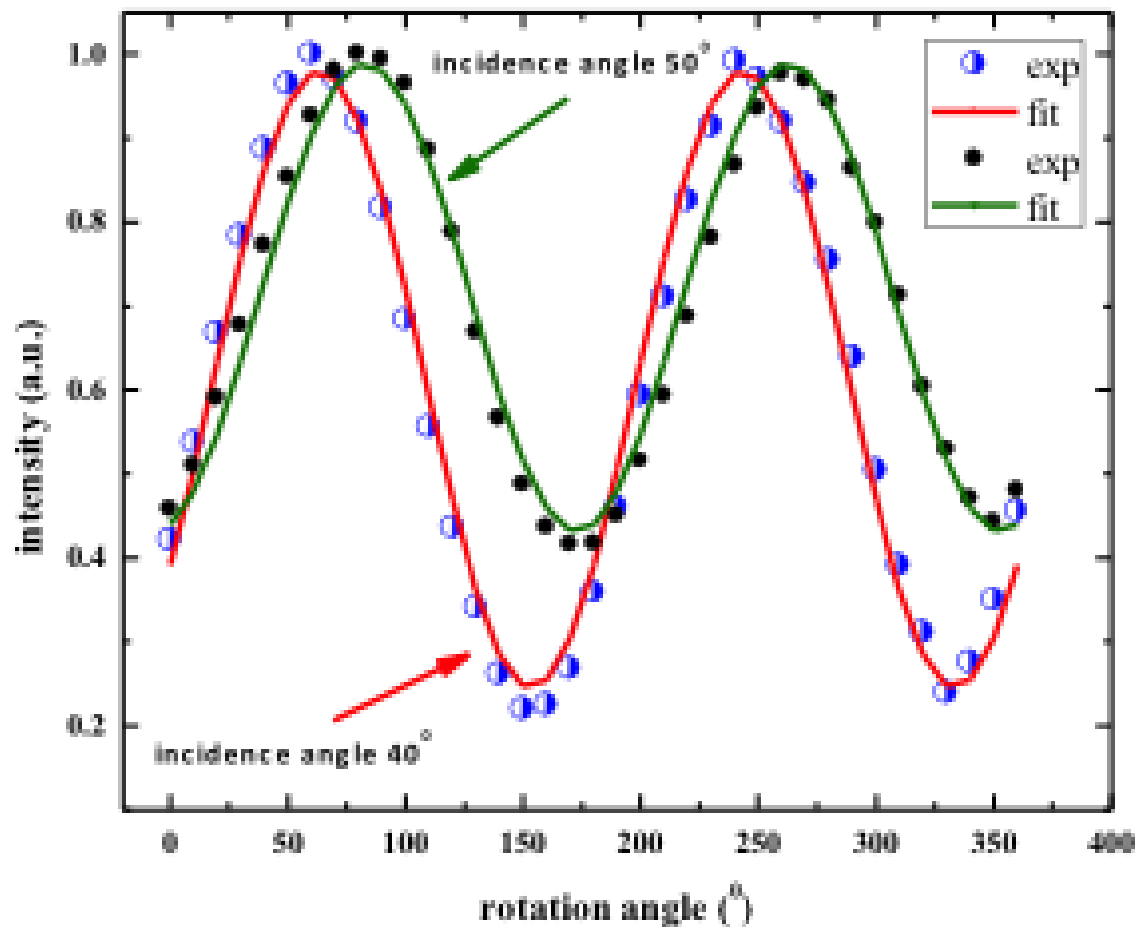
	ratio	phase	ratio	phase	ratio	phase
40	1.20	71	1.10	65	1.12	69 ± 6
50	1.24	98	1.13	92	1.08	101 ± 6
60	1.21	122	1.13	117	0.94	120 ± 6
70	1.14	143	1.09	139	1.04	142 ± 6



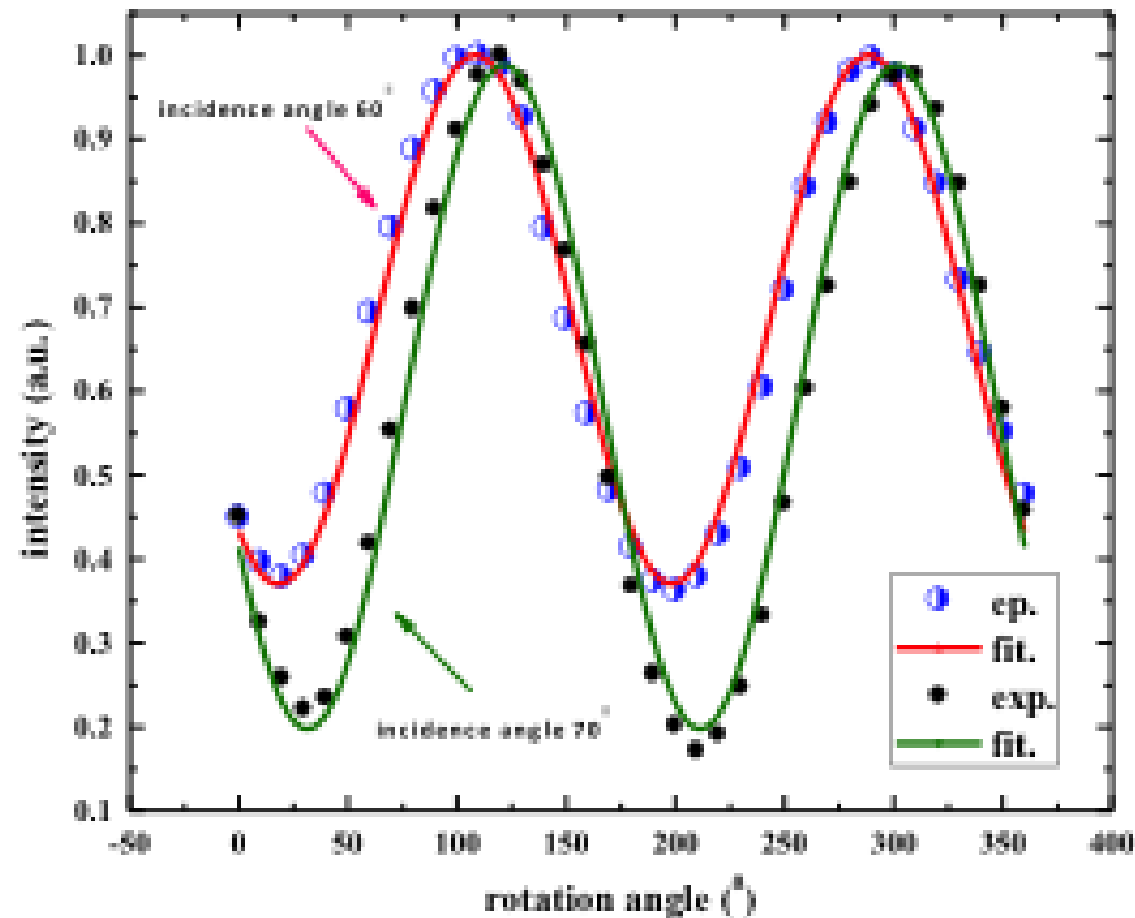
Additionally, we performed the specular reflectance measurements of the sample at the same wavelength to verify the result obtained by analyzing the phase. The figure shows the experimental and the simulated reflectance of the determined structures. In terms of the structure of the sample, the sensitivity in determining the thickness of the aluminum oxide is estimated to be 0.3 nm. Such sensitivity comes out by analyzing the trend of the ratio that requires thinner oxide thickness (2.90 nm instead of 3.18 nm) to be matched.



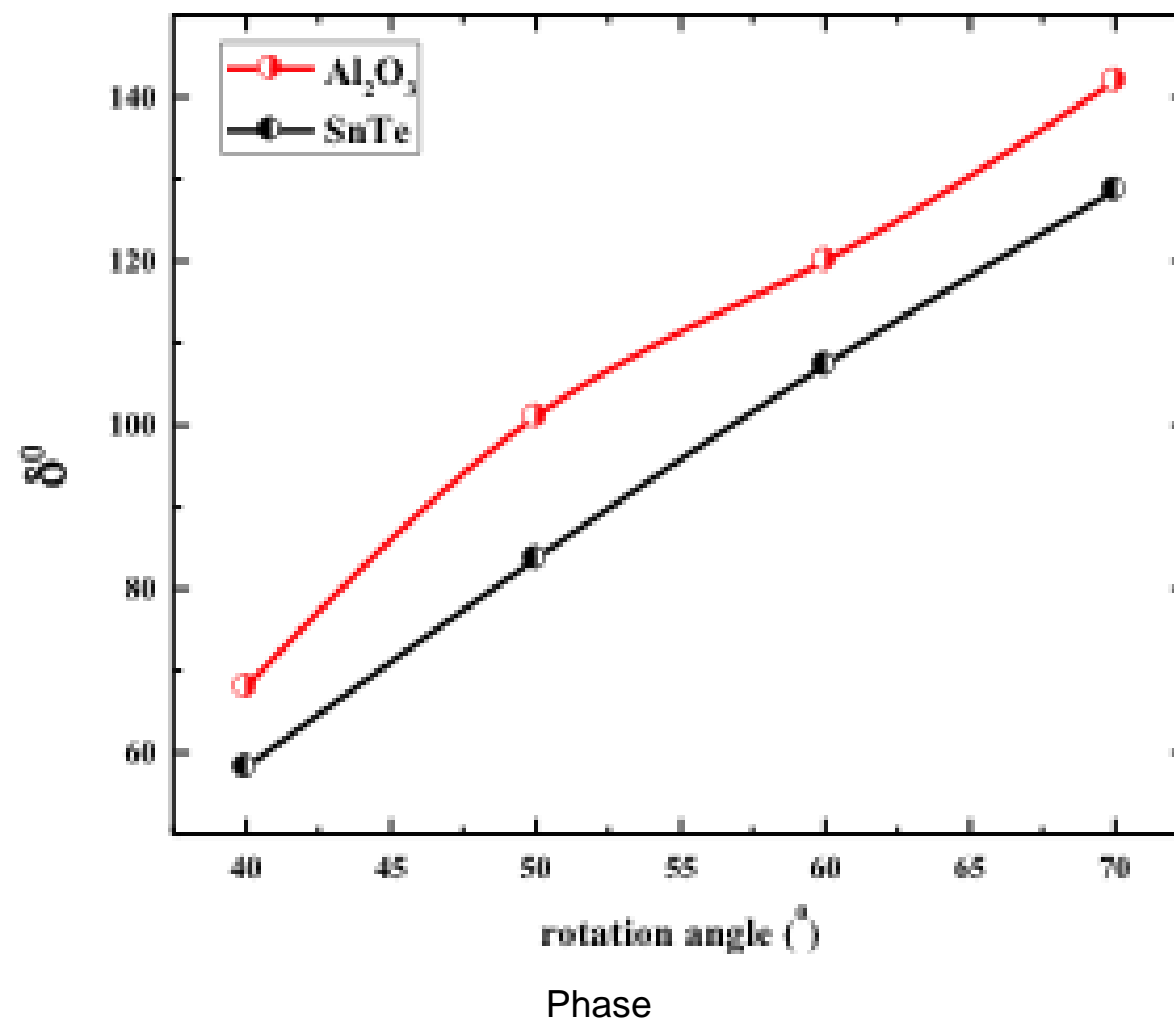
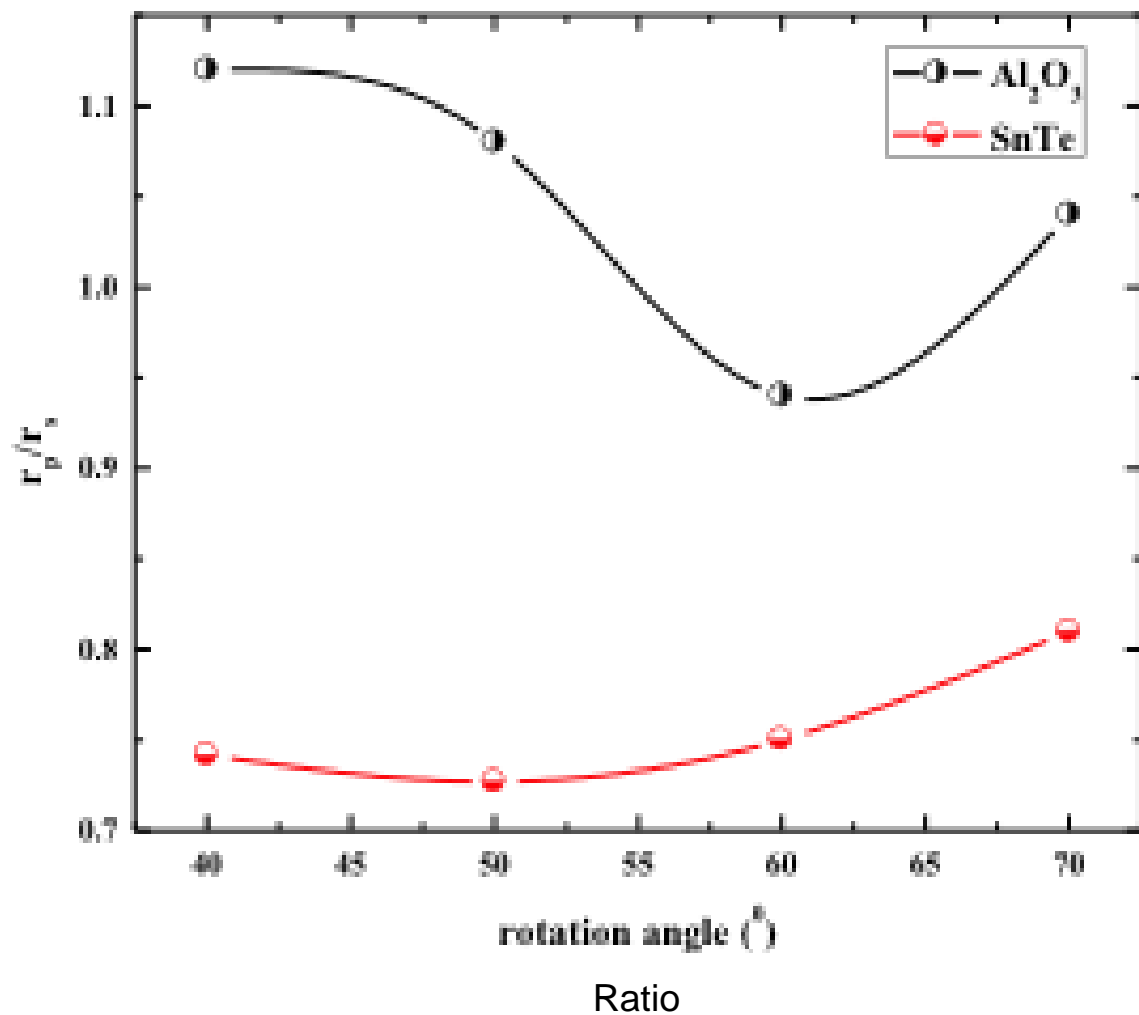
The error in determining the oxide thickness can be reasonably attributed to small variations in optical constants, due to the samples fabrication process and storage, and experimental alignment errors.



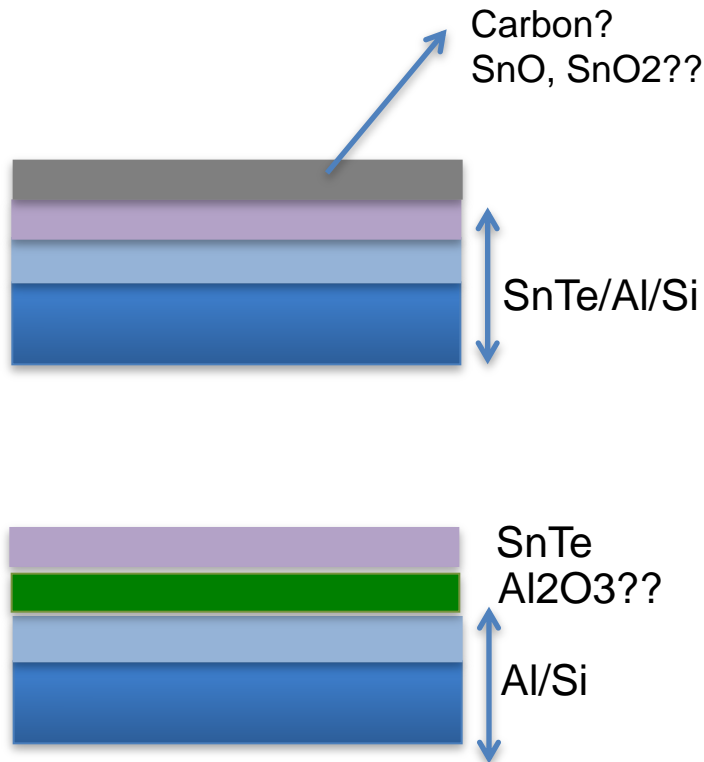
Measured and fitted data of aluminum samples at two different incidence angles 40° and 50°



Measured and fitted curves of aluminum samples at two different incidence angles 60° and 70°



The ellipsometric measurements performed by using the linear polarizer coupled with the EUV reflectometer have been analyzed by using a Matlab code based on the Stokes vectors and Mueller matrix formalism. The code allows to determine phase and ratio (the ratio can be also determined by reflectance measurements).



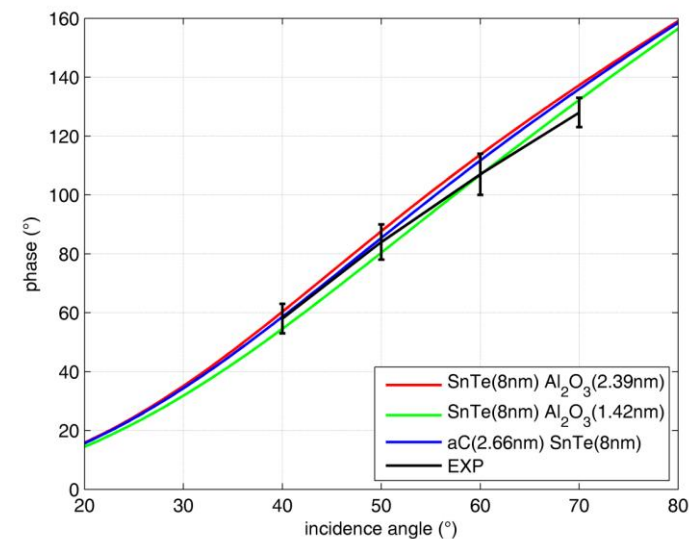
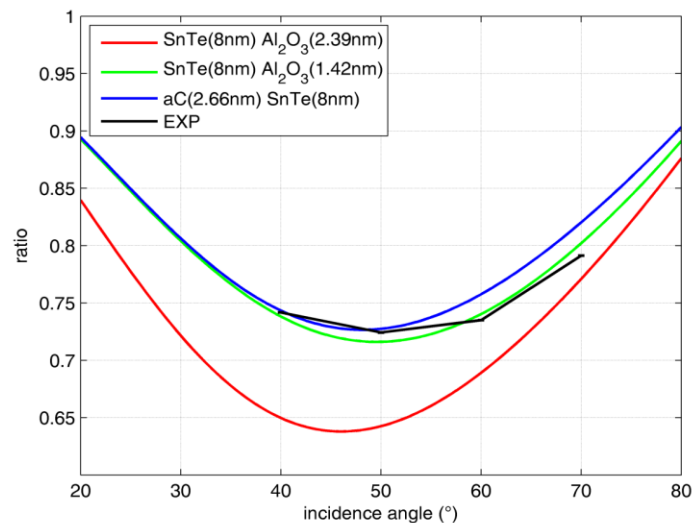
Incidence angle	Fitted data by using ellipsometric measurements (MATLAB code)		Simulation by IMD software nominal structure	
	$\tan\psi = \frac{r_p}{r_s}$	$\Delta\delta^0$	$\tan\psi = \frac{r_p}{r_s}$	$\Delta\delta^0$
40	0.742	58	0.810	47
50	0.724	84	0.785	70
60	0.735	107	0.786	97
70	0.791	129	0.826	124

SnTe(xnm)/Al₂O₃(xnm)/Al(80nm)/Si

Fitted parameter	SnTe (nm)	Al ₂ O ₃ (nm)	χ^2
ratio	7	1.84	0.124
reflectance	7	2.40	0.743
phase	5	1.51	0.592
	6.33 (average)	1.92 (average)	

• *a-C(xnm)/SnTe(xnm)/Al(80nm)/Si*

Fitted parameter	a-C (nm)	SnTe (nm)	χ^2
ratio	2.32	7	0.943
reflectance	2.88	7	0.096
phase	2.50	5	0.703
	2.56 (average)	6.33 (average)	



- Implementation and characterization of the EUV reflectometer facility for polarimetric measurements in 90-160 nm spectral range.
- Designing four reflection EUV linear polarizer in order to be used as a table top EUV ellipsometry system
- The EUV facility was tested to characterize the optical and structural properties of $\text{Al}_2\text{O}_3/\text{Al}$ sample as phase retarder by deriving its amplitude component and phase difference.
- The system can be a very promising laboratory equipment to characterize phase retarders, polarizers and other optics in the EUV region and to investigate the properties of thin films.
- The system can be a simple alternative tool for fast and preliminary experiments compared to measurements sessions at large scale facilities like synchrotron
- Development of QWPs based on Al thin films for the EUV spectral range

